

Constrained Co-evolutionary Metamorphic Differential Testing for Autonomous Systems with an Interpretability Approach

Hossein Yousefizadeh, Shenghui Gu, Lionel C. Briand, *Fellow, IEEE*, and Ali Nasr

Abstract—Autonomous systems, such as autonomous driving systems, evolve rapidly through frequent updates, risking unintended behavioral degradations. Effective system-level testing is challenging due to the vast scenario space, the absence of reliable test oracles, and the need for practically applicable and interpretable test cases. We present CoCoMagic, a novel automated test case generation method that combines metamorphic testing, differential testing, and advanced search-based techniques to identify behavioral divergences between versions of autonomous systems. CoCoMagic formulates test generation as a constrained cooperative co-evolutionary search, evolving both source scenarios and metamorphic perturbations to maximize differences in violations of predefined metamorphic relations across versions. Constraints and population initialization strategies guide the search toward realistic, relevant scenarios. An integrated interpretability approach aids in diagnosing the root causes of divergences. We evaluate CoCoMagic on an end-to-end ADS, InterFuser, within the Carla virtual simulator. Results show significant improvements over baseline search methods, identifying up to 287% more distinct high-severity behavioral differences while maintaining scenario realism. The interpretability approach provides actionable insights for developers, supporting targeted debugging and safety assessment. CoCoMagic offers an efficient, effective, and interpretable way for the differential testing of evolving autonomous systems across versions.

Index Terms—Autonomous systems, autonomous driving systems, system-level testing, metamorphic testing, differential testing, search-based testing, automated testing, cooperative co-evolutionary algorithms.

I. INTRODUCTION

AUTONOMOUS Systems (ASs) are complex software-hardware systems designed to autonomously make real-time operating decisions in open contexts by processing data from a multitude of inputs. These systems are mostly built with Artificial Intelligence (AI) units that learn from vast datasets and may, in the future, continuously evolve through reinforcement learning. As ASs continue to advance, the need for systematic testing becomes increasingly important, to maintain public trust and to satisfy regulatory requirements [1]–[3]. Concurrently, AS development relies on iterative refinement, incorporating new real-world data, optimized network architectures, hyperparameter tuning, and algorithmic tweaks to boost AS performance

Hossein Yousefizadeh and Shenghui Gu are with the School of EECS, University of Ottawa, Canada. E-mails: hyous028@uottawa.ca; sgu2@uottawa.ca

Hossein Yousefizadeh and Shenghui Gu contributed equally to this work.

Lionel C. Briand holds shared appointments with the School of EECS, University of Ottawa, Canada, and the Lero SFI centre for Software Research, University of Limerick, Ireland. E-mail: l briand@uottawa.ca

Ali Nasr is with Waterloo Research Center of Huawei Technologies Canada Co., Ltd., Canada. E-mail: ali.nasr2@huawei.com

across diverse operating conditions [4]–[6]. However, each update can inadvertently introduce changes that undermine previously validated behaviors or functionalities. Assumptions about system behavior or responses that once appeared benign may no longer hold under new or even familiar conditions and may therefore lead to unsafe outcomes. Without systematic testing, such behavioral degradations can remain hidden and compromise system reliability and safety. Consequently, there is an urgent need for effective testing methods that systematically identify critical violations triggered by AS updates, particularly as modern ASs are increasingly built on complex AI models whose behavior can be difficult to predict and verify.

Meeting this need is complicated by the fact that the behavior of ASs across diverse scenarios is both complex and unpredictable, making it difficult to detect degradations and trace their root causes. Variations in environmental conditions, task parameters, and system inputs interact with the uncertainty inherent in Machine Learning (ML) or Deep Learning (DL) models to produce a vast array of possible AS responses. In practice, a single update, whether to the model, the control policy, or the training data, can affect hundreds of interconnected components so that a failure observed in one scenario may originate from a subtle modification elsewhere. Isolating which change triggered the degradation, therefore, requires re-creating and re-evaluating numerous complex test cases, a process that demands extensive computational resources and careful methodological design.

In addition, the main obstacle in testing ASs is the lack of dependable test oracles. This challenge arises from the fact that, in many cases, especially in complex or open-ended scenarios, formal specifications or expected outcomes are either absent or difficult to establish [7], [8]. Unlike traditional software, where a function’s input and output can be precisely defined, ASs often operate in environments where a spectrum of behaviors may be acceptable for a given situation. For instance, a robot navigating a crowded space may choose different but equally valid paths, or an automated control system may apply varying control signals within a safe operating range. Human experts sometimes disagree on the correct maneuver in novel situations, and encoding every nuance of safe and comfortable driving into a fixed rule set is generally infeasible. Without clear pass and fail criteria, automated testing cannot definitively flag deviations as degradations, making it nearly impossible to scale testing across the full range of real-world operating conditions.

Furthermore, even when degradations can be detected without a formal oracle, the practical relevance of such detections

depends heavily on the realism of the scenarios in which they occur. While artificially constructed edge cases can expose system weaknesses, failures observed in realistic scenarios are often of greater practical importance, especially scenarios resembling situations commonly encountered during system execution. Such scenarios are inherently more likely to increase the probability that any detected failure will manifest after deployment. Therefore, prioritizing the discovery of failures in realistic settings enhances the relevance of the testing process and helps focus engineering efforts on risks that are more likely to impact users.

To address these challenges, we propose *Cooperative Co-evolutionary differential and Metamorphic Automated Generator for Interpretable Cases in autonomous systems (CoCoMagic)*, an effective and efficient automated test case generation method that integrates Metamorphic Testing (MT) with Differential Testing (DT) to expose behavioral divergences between AS versions. MT [9] offers a practical approach by evaluating system behavior through Metamorphic Relations (MRs), which define expected relationships between inputs and their corresponding outputs. Instead of verifying absolute correctness, MT checks for consistency across related test cases, making it particularly well-suited for domains such as autonomous driving, where correct behavior is often context-dependent and ambiguous [1], [10], and where labeled data may be insufficient, since it does not require ground-truth outputs for every test case. DT exposes discrepancies by executing multiple versions of a system on the same input and comparing their outputs. In the context of evolving ASs, where system updates may subtly alter behavior, DT coupled with MT can help reveal deviations that violate the expected output relations defined by MRs. Such violations may indicate degradations or unexpected side effects introduced during model fine-tuning or other updates. We cast test case generation as a search problem and seek inputs in which the extent of violation of the expected output relation differs markedly across versions. By systematically discovering such inputs, our method yields effective yet diverse test cases that spotlight safety risks and unintended behaviors introduced during the continuous evolution of ASs. We also incorporate constraints and a population initialization strategy to guide the search toward realistic test cases that reflect real-world conditions. This design ensures that the generated cases are relevant and applicable to practical scenarios, particularly in regions where the updated system is expected to operate but has not yet been thoroughly tested.

To further enhance the utility of *CoCoMagic*, we integrate an interpretability approach that supports the analysis and understanding of the root causes behind the identified behavioral divergences. This approach allows us to analyze the generated test cases and gain insights into the underlying factors contributing to the observed discrepancies, thereby helping developers address potential safety risks more effectively, producing cases that are not only effective at exposing divergences but also understandable and interpretable.

While our method is designed for general applicability to ASs operating in open and complex environments, this work focuses on Autonomous Driving Systems (ADSs) as a representative

and challenging case study. End-to-end ADSs exemplify one of the most complex forms of ASs, positioned at the higher end of the complexity spectrum [11]. To evaluate the effectiveness and efficiency of *CoCoMagic*, we conducted experiments using the CARLA simulator [12] with the INTERFUSER ADS [13]. The results show that *CoCoMagic* significantly outperforms baseline methods in identifying severe behavioral discrepancies, with consistent advantages across a wide range of search budgets and configurations. This superior performance highlights *CoCoMagic* as a promising and scalable solution for testing ADSs. The use of constraints and population initialization effectively guides the search toward realistic and practically relevant test cases, enhancing the applicability of the generated test cases. Moreover, the interpretability approach integrated into *CoCoMagic* enables a detailed analysis of behavioral divergences, offering valuable insights into the underlying factors contributing to the observed discrepancies.

The major contributions of this paper are summarized as follows:

- We proposed *CoCoMagic*, a novel method for automated test case generation that combines MT and DT to expose behavioral divergences between different versions of ASs. We also introduced constraints and a population initialization strategy to guide the search toward realistic test cases that reflect real-world conditions.
- We incorporated an interpretability approach into *CoCoMagic* to facilitate the analysis and understanding of the root causes behind the identified behavioral divergences.
- We applied *CoCoMagic* to a complex case study utilizing an industry-grade simulator and a high-performing ADS.
- We provided a comprehensive evaluation of *CoCoMagic* through large-scale experiments and comparisons against baseline methods, showing its ability to identify behavioral discrepancies and highlight potential safety risks introduced by updates.

CoCoMagic builds on our previous work [14] and mainly differs from it by focusing on efficiently and effectively testing and analyzing updates across system versions. The key differences are as follows:

- *CoCoMagic* is specifically designed to systematically detect behavioral divergences between different versions of ASs, rather than focusing solely on testing a single version.
- It incorporates constraints and a population initialization strategy to guide the search toward test cases that are realistic and reflective of real-world conditions.
- It integrates an interpretability approach that facilitates understanding of the root causes behind observed behavioral divergences through analysis of the generated test cases.

The remainder of this paper is organized as follows. Section II introduces the key challenges and formally defines the problem. Section III reviews related research and highlights existing gaps. Section IV presents a detailed description of *CoCoMagic*. Section V reports the empirical evaluation of the proposed approach. Section VI analyzes the results and

discusses potential threats to validity. Finally, Section VII summarizes the paper and outlines future work directions.

II. PROBLEM AND CHALLENGES

In this section, we outline the key challenges associated with testing versions of ASs and the need for a systematic approach to address these challenges. We begin by defining the problem, followed by a discussion of the specific challenges that arise in this context.

The primary problem to be addressed in this research is the development of an automatic, effective, and time-efficient system-level testing methodology for an updated AS to identify scenarios where its behavior has improved or declined compared to the original version.

However, assessing the impact of updates presents several challenges:

- **Scalability and Coverage.** Thoroughly testing ASs in all conditions is infeasible due to the vast space of possible execution scenarios. Many factors influence AS behavior, such as road conditions, weather, traffic dynamics, and pedestrian interactions in the case of ADSs. Ensuring that the testing framework effectively captures the full range of behavioral changes between the original and updated versions is a significant challenge. Without comprehensive coverage, some critical failure cases may go undetected, leading to potential safety risks.
- **Oracle Problem.** Determining whether a behavioral change in the AS constitutes an improvement or a decline is non-trivial. For example, tasks in ADSs, including perception, planning, and decision-making, are highly complex, and their correctness cannot usually be defined explicitly and precisely. The unpredictable nature of real-world traffic conditions further complicates this problem, making it difficult to establish ground-truth expectations for every possible scenario. The absence of well-defined test oracles can lead to ineffective evaluations, as it becomes challenging to distinguish between beneficial adaptations and unintended degradations.
- **Scenario Realism.** While artificially constructed edge cases can reveal vulnerabilities, failures found in realistic scenarios, particularly those closely resembling situations already encountered during system execution, are often of greater practical importance. Such scenarios are inherently more likely to occur in deployment, meaning that any detected failure poses a higher operational risk. Therefore, guiding the testing process toward realistic conditions enhances the relevance of test results, ensuring that identified violations reflect risks that are plausible in practice rather than purely theoretical.
- **Interpretability.** ASs rely on ML or DL-based components with a vast number of parameters and intricate decision-making mechanisms. Fine-tuning involves modifying these parameters to optimize performance, but understanding how these modifications influence overall system behavior is not straightforward. Without systematic and well-designed testing methodologies, it is difficult to diagnose issues and ensure that the system changes align with expected improvements.

- **Time Constraints.** In many scenarios, fine-tuning occurs automatically and frequently, particularly in self-adaptive systems that continuously refine their models. Given the rapid pace of such updates, an efficient testing process is essential. The challenge is to develop an automated and fast testing approach that provides insights into AS behavioral changes without significantly delaying deployment.

Addressing these challenges is critical to ensuring the safety of updated AS. A robust testing methodology should be capable of efficiently identifying behavioral changes, overcoming the oracle problem, enabling interpretability, and operating within realistic time constraints.

Specifically, we re-express the problem as a search problem. Let \mathcal{S} denote the space of all possible operating scenarios, and let \mathcal{Q} denote the space of all possible perturbations derived from a set of MRs that share the same output relation *or*. We define a function $\Delta E_{or}(s, q)$ that quantifies the difference in the extent of MR violation of *or* between two versions of an AS, given a source scenario $s \in \mathcal{S}$ and its follow-up scenario $q(s)$, which results from applying perturbation $q \in \mathcal{Q}$ to s . For illustration, consider a testing context where the goal is to evaluate how different versions of an ADS behave when encountering a pedestrian under various weather conditions. The space \mathcal{S} includes all possible scenarios defined by factors such as road geometry, traffic density, and initial pedestrian placement. The space \mathcal{Q} includes possible perturbations, such as changes in weather (e.g., fog or rain), derived from an MR expecting the ADS to reduce speed when visibility decreases. Now, given a source scenario $s \in \mathcal{S}$ with clear visibility, applying a perturbation $q \in \mathcal{Q}$ yields a follow-up scenario $q(s)$ with reduced visibility. The function $\Delta E_{or}(s, q)$ then measures how inconsistently the two ADS versions respond to the same visibility change, specifically quantifying the difference in the extent to which they violate the expected speed reduction behavior defined by *or*. A larger value indicates greater inconsistency between system versions in meeting the expected MRs.

Definition 1 (Problem). The problem is to find a diverse set \mathcal{SP} of scenario-perturbation pairs $(s, q) \in \mathcal{S} \times \mathcal{Q}$ such that the extent of violation of the expected output relation *or* differs between two versions of the AS when applied to the same perturbed scenario $q(s)$:

$$\mathcal{SP} = \{(s, q) \in \mathcal{S} \times \mathcal{Q} \mid \Delta E_{or}(s, q) > 0\}$$

III. RELATED WORK

This section reviews prior work in two main areas that intersect with our contributions, i.e., Search-based Testing of ASs and Metamorphic Testing of ASs.

A. Search-based Testing of Autonomous Systems

Search-based testing has emerged as a key strategy for the system-level evaluation of ASs across a range of domains, including autonomous vehicles, aerial drones, robotic platforms, and other complex multi-input AI-based systems. The central idea is to automate the exploration of complex,

high-dimensional scenario spaces using evolutionary search to uncover failure-inducing behaviors.

Ben Abdessalem et al. [15] pioneered a multi-objective strategy that combines search-based testing with surrogate models based on neural networks to assess advanced driver assistance systems in simulation. In subsequent works, the authors extended their approach to detect conflicts between automated system functions [16] and to test vision-based control systems [17], demonstrating that their methods uncovered substantially more critical scenarios than baseline techniques. Dreossi et al. [18] proposed a compositional search-based framework tailored for ML-enabled ADSs, leveraging constraints from both perception and system input spaces to isolate counterexamples efficiently. Sartori [19] proposed a simulation-based testing framework for autonomous robots that leverages search-based techniques to guide the generation and selection of virtual test worlds, incorporating test objectives, prior results, and dynamic agents. Through two industrial case studies involving mobile robots, the approach demonstrated its capability to reveal safety-critical failures efficiently, even in low-fidelity simulations. Haq et al. [20] introduced *SAMOTA*, which employs many-objective optimization with surrogate models to efficiently surface safety violations by approximating expensive simulations. Kolb et al. [21] developed a set of fitness function templates tailored for search-based testing of ADSs in intersection scenarios. This work extended earlier efforts on highway environments [22] and showed that tailored fitness definitions can significantly improve the generation of diverse and safety-relevant tests compared to random testing baselines. Luo et al. [23] presented *EMOOD*, a search-based framework that leverages evolutionary strategies to systematically uncover test scenarios involving compound violations of system requirements. Birchler et al. [24], [25] proposed test case prioritization strategies aimed at optimizing the fault detection efficiency in regression testing. Their empirical results demonstrated that their approach can enhance early fault detection and testing efficiency relative to baseline methods. Khatiri et al. [26] proposed *SURREALIST*, a search-based testing framework for Unmanned Aerial Vehicles that generates simulation test cases in the neighborhood of real flight logs by first replicating and then smoothly perturbing recorded trajectories. Their approach uncovered unstable and potentially unsafe system behaviors that did not occur in the original logs, improving the realism and fault-detection capability of simulation-based tests. Shimanuki et al. [27] proposed *CORTEX-AVD*, a framework that integrates CARLA and SCENIC [28] with a genetic algorithm to automatically generate corner cases from textual scenario descriptions using a multi-factor fitness function. Their results showed that *CORTEX-AVD* significantly increased the generation of high-risk events and improved simulation utility compared to random sampling.

Fuzzing techniques have also been employed to trigger faulty behaviors by systematically perturbing operating scenarios. Li et al. [29] introduced *AV-Fuzzer*, which leverages genetic algorithms to perturb traffic participants in the APOLLO platform [30], leading to broader discovery of critical safety violations compared to methods such as random fuzzing or

adaptive stress testing. Cheng et al. [31] proposed *BehAVExplor*, a behavior-guided fuzzing approach that uses unsupervised clustering to model ego vehicle behavior and guide scenario generation based on behavior diversity and violation potential. Evaluated on APOLLO and LGSVL [32], it outperformed state-of-the-art baselines by detecting a significantly larger and more diverse set of violations. Crespo-Rodriguez et al. [33] proposed *PAFOT*, a position-based framework that models non-playable character maneuvers using a nine-position grid around the ego vehicle and applies a genetic algorithm to evolve collision-inducing scenarios. To improve local search, *PAFOT* incorporates a mutation-based local fuzzing strategy, which helps uncover additional safety violations near high-risk cases, leading to better performance than *AV-Fuzzer* and random testing in CARLA. In a more recent study, Ji et al. [34] proposed *DoFuzz*, a search-based framework that generates kinematically valid and naturalistic driving scenarios using a hybrid physics-based and learning-based encoding, and prioritizes test executions based on a freshness score that estimates behavioral novelty. Evaluated on multiple CARLA *Leaderboard* [35] driving tasks, *DoFuzz* discovered more unique failures and achieved faster convergence compared to *BehAVExplor*.

Algorithmic innovations have further enriched the field. Gambi et al. [36] integrated search-based testing with *Procedural Content Generation*, which is a technique for algorithmically creating diverse virtual environments, to automatically construct virtual road scenarios for testing lane-keeping functionalities. Goss and Akbaş [37] applied the *Eagle Strategy*, alternating between broad sampling and focused local search to hone in on critical areas. Zheng et al. [38] proposed a quantum genetic algorithm to reduce the computational load associated with population size. Humeniuk et al. [39] introduced *AmbieGen*, a modular search-based test generation framework that uses evolutionary algorithms to identify fault-revealing scenarios for ADSs and robots. Through extensive evaluations on lane-keeping assist systems and obstacle-avoiding robots, their method revealed significantly more failures compared to the baseline methods. In a subsequent study, they proposed *RIGAA* [40], a reinforcement learning-informed genetic algorithm that integrates a pre-trained reinforcement learning agent into the evolutionary search process to improve the efficiency of simulator-based test generation. Evaluated on autonomous robot and vehicle systems, *RIGAA* significantly outperformed prior methods, including *AmbieGen*, revealing more failures in the vehicle domain and achieving faster convergence in both scenarios.

A recent line of work explores using multiple simulators to improve the robustness and generalizability of test results. Biagiola et al. [41] introduced the *Digital Siblings* approach, which leverages an ensemble of general-purpose simulators to jointly approximate the behavior of a digital twin through cross-simulator test generation, migration, and failure agreement analysis. Their evaluation showed that this multi-simulator setup more accurately predicts failures on a digital twin than any individual simulator alone, supporting the case for ensemble-based simulation in ADS testing. Building on this idea, Sorokin et al. [42] proposed *MultiSim*, a search-based

testing framework that integrates multiple simulators directly into the test generation loop to identify simulator-agnostic, failure-inducing scenarios. Compared to single-simulator testing and *Digital Siblings*, *MultiSim* significantly improved the validity rate of failures and detected more simulator-agnostic failures while maintaining comparable efficiency.

While most search-based methods focus on exploring variations in environmental or scenario parameters, a few studies have begun to examine the impact of internal AS configuration parameters. For example, Pan et al. [43] proposed *SafeVar*, a search-based approach that identifies minimal variations in vehicle characteristics, such as mass, brake torque, and tire friction, that can significantly compromise ADS safety. Using *NSGA-II* algorithm [44], *SafeVar* consistently generated critical parameter settings that induced unsafe behavior across multiple scenarios and ADS models, outperforming random search in both effectiveness and efficiency.

In summary, search-based testing has proven highly effective in uncovering critical failures in ASs by systematically exploring scenario spaces and guiding test generation toward high-risk behaviors and thereby surfacing edge cases. Techniques in this domain have evolved from early multi-objective formulations and surrogate-assisted search to more recent innovations involving fuzzing, behavioral clustering, and multi-simulator coordination. Despite these advancements, search-based testing remains computationally expensive, particularly when dealing with high-dimensional scenario parameters, complex operating scenarios, and high-fidelity simulations. This cost becomes a critical bottleneck in modern AS development pipelines, where systems are frequently retrained, fine-tuned, or updated to adapt to new data, hardware, or operating environments. These challenges highlight the need for scalable and adaptive testing frameworks that can efficiently identify critical behavioral changes across AS versions, minimize redundant simulation efforts, and keep pace with the rapid development cycles of modern ASs.

B. Metamorphic Testing of Autonomous Systems

Metamorphic Testing (MT) [9], [45] was introduced as a solution to the test oracle problem in domains where ground-truth output is hard to define. Recent work highlights the effectiveness of MT in many domains, including AS, where it enables the detection of failures by checking the consistency of outputs across related inputs rather than relying on a known ground truth [46].

At the module level, MT has been extensively applied to assess the dependability and robustness of perception systems. For instance, Yang et al. [47] introduced *MetaLiDAR*, an automated MT framework that employs object-level manipulations, such as insertions, deletions, and affine transformations, to produce realistic variants of point cloud data for evaluating LiDAR-based object detection. They later proposed *MetaSem* [48], a framework based on semantic-level modifications to driving scenes (e.g., changes to traffic signs and road markings), revealing additional inconsistencies missed by prior methods. Zhou and Sun [10] illustrated that injecting even minor perturbations outside the region of interest in LiDAR data

could lead to critical perception errors, such as missed obstacles, underscoring the vulnerability of perception modules.

Beyond the module level, MT has also gained traction for system-level testing. Lindvall et al. [49] developed a simulation-based testing framework that integrates MT with model-based testing to automatically generate and evaluate test cases for autonomous drones under variations of geometric and environmental conditions. Their approach revealed unstable behaviors and critical failure cases, including collisions and perception failures, demonstrating its effectiveness in uncovering subtle flaws that traditional methods often miss. Tian et al. [50] introduced *DeepTest*, which defines transformation-based MRs involving lighting and weather variations to identify behavioral inconsistencies in Deep Neural Network-based ADSs. This idea was expanded in *DeepRoad* [51], which applied generative adversarial networks to generate high-fidelity weather conditions, enabling more realistic and effective scenario transformations. Pan et al. [52] proposed an MT framework that focused on fog-related driving conditions, using variations in fog density and direction to evaluate performance. Han and Zhou [53] employed a metamorphic fuzzing approach, using MRs to filter false positives by identifying genuine faults among automatically generated edge-case scenarios. In a more recent effort, Cheng et al. [54] developed *Decictor*, a scenario-based MT framework aimed at assessing optimal decision-making in ADSs. By applying non-invasive mutations to the driving environment, *Decictor* identifies situations where the system diverges from the optimal trajectory without altering the ground-truth path. Fredericks et al. [55] proposed *DroneMR*, an MT framework for software-defined drone systems that combines evolutionary search with contextual MR inference to detect failures under uncertain conditions. Applied to a micro-drone platform in simulation, *DroneMR* successfully generated diverse operating contexts and corresponding metamorphic test cases, demonstrating its potential for both design-time and run-time validation in safety-critical settings.

Overall, MT provides a practical means to detect failures in both module-level and system-level testing of ASs, especially in the absence of a test oracle. Its power lies in the definition of MRs that express consistent behavioral expectations under controlled input modifications, enabling the detection of latent inconsistencies. Nonetheless, one major limitation lies in the difficulty of formulating comprehensive and safety-relevant MRs, especially in dynamic, real-world operating scenarios characterized by environmental variability and unpredictable agent interactions. The task of identifying effective MRs often requires significant domain expertise and manual effort, making automation a persistent open challenge [56]. However, given that MRs encode general behavioral properties rather than exact output specifications, they can still be effective even when only partially specified, as violations of these MRs may still indicate anomalous or flawed behaviors.

C. Discussion

The current body of research identifies search-based testing and MT as the two principal methodologies for system-level evaluation of ASs. Search-based testing has proven effective

in systematically exploring large and complex scenario spaces to uncover rare but safety-critical failures, benefiting from advancements including surrogate modeling, behavior-guided fuzzing, and other innovative approaches. On the other hand, MT has emerged as a practical solution to the oracle problem, enabling validation in scenarios where ground-truth outputs are unavailable by checking the consistency of outputs under controlled input transformations defined by MRs.

Despite the progress achieved by existing techniques, several limitations remain that hinder their practical deployment in real-world AS development cycles. Most notably, current search-based approaches are computationally expensive, requiring extensive simulation time and resources to explore high-dimensional scenario spaces. This limitation becomes especially problematic in modern development settings, where ASs are continuously updated to accommodate new environments, system configurations, or operating policies. In such contexts, the cost of re-running full-scale test campaigns after each system update is prohibitive. Furthermore, current approaches assess ASs in isolation, so they cannot reveal whether a newly discovered failure is a longstanding flaw or a degradation introduced by the latest software update. This inability to distinguish degradations from persistent issues makes it difficult for developers to prioritize fixes, allocate debugging resources effectively, and assess the impact of recent updates on system safety. Finally, existing methods typically lack mechanisms for fault interpretability, offering little insight into why failures occur or which scenario attributes contribute most to induce unsafe behaviors. This lack of explanatory power limits their utility in iterative development, where actionable feedback is essential for effective debugging and refinement.

Building on these observations, our work investigates how search-based testing and MT can be integrated into a unified framework that addresses the practical limitations of current approaches. The central question we explore is how to design a testing methodology that remains effective and efficient in uncovering critical behavioral failures induced by system updates, while also providing insights into the key attributes of failure-inducing scenarios.

IV. OUR APPROACH

In this section, we present our solution to the problem outlined in Section II. Our approach combines constrained Cooperative Co-Evolutionary Algorithm (CCEA) with DT and MT to generate test cases that expose differences in MR violations between two versions of an AS. CCEA decomposes the original high-dimensional search into lower-dimensional subproblems, each handled by an independent population, not only enabling parallelism but also increasing the efficiency of the search process [57]. Specifically, we cast the problem as a two-population CCEA: the first population explores source scenarios, and the second consists of perturbations derived from the predefined MRs. Through collaboration, individuals from both populations combine to form complete test cases, i.e., complete solutions, that reveal differences in MR violations. To guide the search, we use a set of MRs that share the same output relation, allowing the search to explore a broader and

more diverse range of test cases while ensuring that every candidate test case directly targets relevant relation violations.

In the following sections, we first define the representations for MRs, scenarios, and perturbations used in our approach (Section IV-A). Next, we introduce a fitness evaluation framework (Section IV-B), which incorporates a joint fitness function [58], [59] for measuring the difference in MR violations in complete solutions formed through collaboration between individuals from the two populations, as well as an individual fitness function [58], [59] for assessing each individual's contribution. To ensure that every solution remains applicable to real-world conditions, we also incorporate constraints into the search process (Section IV-C). We then present our method based on constrained CCEAs, which leverages the defined representations, fitness functions, and constraints to guide the search effectively (Section IV-D). Finally, we describe the root cause analysis applied to the generated complete solutions, which helps interpret and explain the observed differences in MR violations between the two AS versions (Section IV-E).

A. Representations

In this subsection, we first describe how MRs are represented in our search framework. We then introduce the two co-evolving populations: one representing source scenarios and the other representing perturbations derived from a predefined set of MRs. Each perturbation is applied to a source scenario to generate a corresponding follow-up scenario.

An MR generally specifies a relation \mathcal{R} that defines a relationship between a sequence of inputs and their respective outputs [9]. In the most common form, an MR consists of two components: an input relation ir and an output relation or . The input relation ir specifies how two inputs x_1 and x_2 are related, while the output relation or describes the expected relationship between their outputs $f(x_1)$ and $f(x_2)$ [60], where f represents the function or system under test. The relation \mathcal{R} holds when both ir and or are satisfied, and can be formally expressed as:

$$\mathcal{R}(x_1, x_2, f(x_1), f(x_2)) := ir(x_1, x_2) \wedge or(f(x_1), f(x_2))$$

This formulation allows an MR to be interpreted as a consistency rule that governs how the system's output should change in response to a defined transformation of its input. In our work, we formally define an MR as a tuple $mr := (ir, or)$. Given the input relation ir providing an abstract specification of how a source scenario can be transformed, we can derive concrete metamorphic transformations that modify the attributes of a source scenario to produce a follow-up scenario. A violation occurs when the follow-up scenario satisfies ir , but the corresponding outputs fail to satisfy or , indicating that the MR has been violated. In our search framework, we employ a set of MRs that share a common output relation or to guide the search, which can be defined as $MR := \{mr_i = (ir_i, or) \mid i \in \mathbb{N}^*\}$.

A scenario s can be formally represented as a vector composed of real and integer values. In practice, the specific vectorization scheme depends (in part) on the observable and controllable elements of the underlying system or simulator. For example, in the context of ADSs, a scenario typically includes the ego vehicle, its trajectory, environmental factors

(e.g., weather), and both dynamic (e.g., other vehicles and pedestrians) and static (e.g., obstacles) objects [61], [62]. Each of these elements is characterized by multiple attributes of different types, including continuous values and categorical variables encoded as integers. All attributes are constrained within predefined ranges that reflect realistic and valid conditions.

A perturbation can be formally defined as a sequence of metamorphic transformations, denoted as $q := \langle c_1, c_2, \dots, c_k \rangle$, which are applied sequentially to a source scenario s to produce a follow-up scenario $q(s)$. Each transformation c_i in q corresponds to a unique input relation ir_i from the given set of MRs. Typically, a transformation c_i may represent a modification to the source scenario, such as adding a new object, removing an existing one, or replacing an existing object with a new one. It may also represent no change at all, where no modification is applied for that specific transformation. This flexible structure allows perturbations to be constructed selectively, so that not every available transformation needs to be included. However, we require that at least one actual transformation be applied in order to produce a follow-up scenario with meaningful variation.

B. Fitness Function

We aim to define fitness functions that effectively guide the search toward solutions that maximize the difference in MR violations between two versions of an AS. To this end, we first introduce a method for quantifying the extent of MR violation between a source and a follow-up scenario. We then extend this definition to compute the difference in MR violations between two versions of the AS.

Definition 2 (Extent of MR violation). Given a system under test V , a source scenario s and a perturbation q derived from a set of MRs that share the same output relation or , and a function D_{or} which quantifies the deviation from or , we define the extent of violation of or as follows:

$$E(s, q, V, D_{or}) := D_{or}(V(s), V(q(s))) \quad (1)$$

where $V(s)$ and $V(q(s))$ denote the outputs produced by the system V when executing the source scenario s and the follow-up scenario $q(s)$, respectively. The exact formulation of D_{or} depends on the specific or of the MR in use and thus the extent of violation is computed accordingly. For example, if or specifies that the output time series of the ego vehicle's speed should remain unchanged between the source and follow-up scenarios, D_{or} can be defined as the mean of the squared differences between each corresponding point in the two speed series. Eq. (1) captures how much the behavior in the follow-up scenario deviates from what is expected. A higher value indicates a greater deviation, suggesting a more significant violation of the metamorphic relation. In Eq. (1), the pair (s, q) constitutes a complete solution.

Definition 3 (Difference in MR violations). Given a source scenario s and a perturbation q derived from a set of MRs with the same output relation or , and two versions of an AS, denoted V_{ref} and V_{test} , the difference in MR violation between the two versions is defined as follows:

$$\begin{aligned} \text{Diff}(s, q) := & |\max(E(s, q, V_{test}, D_{or}), 0) - \\ & \max(E(s, q, V_{ref}, D_{or}), 0)| \quad (2) \end{aligned}$$

We use the maximum of E and 0 to ignore negative values of E , which indicate no violation of the given MRs. In such cases, the difference is not meaningful and should not influence the fitness. Eq. (2) quantifies how differently the two system versions respond to the same set of MRs, highlighting changes that strengthen or alleviate MR violations. In our framework, Diff serves as the joint fitness function, which we aim to maximize during the search process to identify complete solutions that best expose behavioral discrepancies between the two versions.

To guide the optimization of each population independently, we define an individual-level fitness function that captures how well a given scenario or perturbation contributes to the discovery of differences in MR violations. This function assesses each individual based on its best-performing collaboration with members of the opposite population. For a source scenario, its fitness is computed as the highest violation difference it produces when paired with any perturbation from the current population. Conversely, for a perturbation, its fitness corresponds to the maximum violation difference observed across all source scenarios with which it is combined.

Definition 4 (Individual Fitness Function). Formally, given an individual i , its fitness is defined as follows:

$$\text{fitness}(i) := \begin{cases} \max_j (\text{Diff}(i, q_j)) & \text{if } i \text{ is a scenario} \\ \max_j (\text{Diff}(s_j, i)) & \text{if } i \text{ is a perturbation} \end{cases} \quad (3)$$

where each q_j or s_j is drawn from the opposite population.

This approach encourages individuals to specialize in combinations that are most likely to reveal behavioral differences between system versions. Prior work has shown that relying on the maximum fitness obtained with collaborators, rather than the average or minimum, leads to more effective co-evolutionary outcomes [59], [63]–[65].

C. Constraints

The updated version of an AS is typically retrained to adapt to changes in its operating environment. As a result, it may be exposed to new environmental conditions that were absent or insufficiently tested in the previous version. To ensure the system's reliability and safety under these new conditions, it is essential to evaluate its behavior accordingly. To this end, we impose constraints on the search process to guide test case generation toward scenarios that reflect these newly introduced conditions. Specifically, the search is constrained to generate complete solutions that are not only effective in revealing differences in MR violations but also aligned with those new operating conditions observed in execution time, referred to as execution scenarios. These execution scenarios represent specific, real-world situations newly encountered by ASs during actual operation. They are collected at runtime through monitoring mechanisms integrated

into ASs and encompass a wide range of situations, such as varying road geometries, traffic densities, and environmental conditions, providing a realistic and representative basis for testing.

To enforce relevance, we quantify how similar a generated complete solution is to these real-world execution scenarios by measuring its dissimilarity to a set of execution scenarios \mathbb{S} collected beforehand. This helps focus the search on solutions that are both meaningful and realistic, ensuring that the generated test cases reflect conditions the system is likely to encounter in practice.

Definition 5 (Dissimilarity to execution scenarios). Given a source scenario s , a perturbation q derived from a set of MRs sharing the same output relation, and a set of execution scenarios \mathbb{S} , the dissimilarity of the complete solution formed by s and q to \mathbb{S} is defined as:

$$Dissim(s, q, \mathbb{S}) := \min_{i \in \{s, q(s)\}} \left(\min_{j \in \mathbb{S}} (dist(i, j)) \right) \quad (4)$$

where $q(s)$ denotes the follow-up scenario and $dist(i, j)$ represents a distance measure between scenarios i and j . A typical choice for $dist$, which accommodates both continuous and categorical variables, is the heterogeneous distance metric [66]. Eq. (4) measures how dissimilar a complete solution is from the set \mathbb{S} by considering the minimum distance between either the source or follow-up scenario and its nearest neighbor in \mathbb{S} . This approach ensures that at least one component of each complete solution closely resembles a real execution scenario from \mathbb{S} , preserving relevance. Using the minimum rather than the average distance avoids inflating dissimilarity when a complete solution is very close to one scenario but far from others, which can result in a misleadingly moderate average that suggests the solution is farther from the set than it actually is. This constraint helps maintain the plausibility and practical relevance of the generated test cases, focusing the search on behavior differences that are not only theoretically interesting but also applicable in real-world AS deployments.

D. Algorithm

Building on the representations introduced in Section IV-A, the fitness functions defined in Section IV-B, and the constraints described in Section IV-C, this section presents our proposed algorithm, *Cooperative Co-evolutionary differential and Metamorphic Automated Generator for Interpretable Cases in autonomous systems (CoCoMagic)*. The overall workflow is illustrated in Fig. 1. Our approach integrates a constrained archive-based CCEA with DT and MT to effectively and efficiently explore high-dimensional and complex search spaces. *CoCoMagic* decomposes the search space into two interacting populations, i.e., scenarios and perturbations, enabling them to evolve independently while collaborating to form complete solutions. The search is guided by a predefined set of MRs, which help address the oracle problem by providing structured evaluation criteria and improve search efficiency by focusing on behavior differences that matter across system versions. Additionally, the constraints applied in *CoCoMagic* ensure

Algorithm 1: Cooperative co-evolutionary algorithm.

```

Input: Population size  $n$ 
        Execution scenarios  $\mathbb{S}$ 
Output: Archive of complete solutions  $X$ 

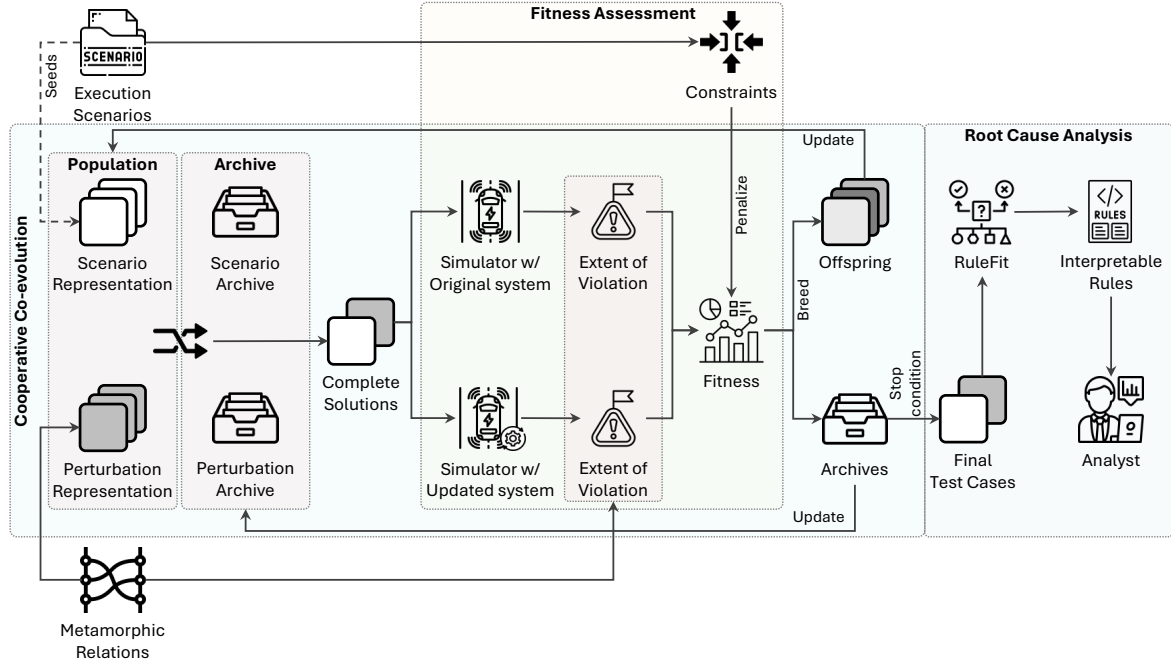
1 Population of scenarios  $P_s \leftarrow initPopulation(n);$ 
2 Population of perturbations  $P_q \leftarrow initPopulation(n);$ 
3 Archive of scenarios  $X_s \leftarrow P_s;$ 
4 Archive of perturbations  $X_q \leftarrow P_q;$ 
5 Archive of complete solutions  $X \leftarrow \emptyset;$ 
6 while not(stopping condition) do
7    $P_s, P_q, X \leftarrow assessFitness(P_s, P_q, X_s, X_q, X, \mathbb{S});$ 
8    $X_s \leftarrow updatePopulationArchive(P_s);$ 
9    $X_q \leftarrow updatePopulationArchive(P_q);$ 
10   $P_s \leftarrow breed(P_s) \cup X_s;$ 
11   $P_q \leftarrow breed(P_q) \cup X_q;$ 
12 end
13 return  $X;$ 

```

that the generated complete solutions remain as relevant and realistic as possible in the context of actual execution scenarios.

Algorithm 1 presents the pseudocode of our algorithm. It takes as input a population size n and a set of execution scenarios \mathbb{S} , and it outputs an archive X containing distinct complete solutions. The algorithm begins by initializing two populations: a scenario population P_s , which is either randomly generated or sampled from \mathbb{S} (line 1), and a perturbation population P_q (line 2). Sampling the scenario population from execution scenarios enhances both the diversity of the initial population and its relevance to real-world conditions. The choice of initialization strategy influences the similarity of the resulting complete solutions to real-word scenarios, as further discussed in Section V-E. Corresponding population archives X_s and X_q are created at lines 3 and 4. An empty archive of complete solutions X is also initialized at line 5. The core of the algorithm is a co-evolutionary process where P_s and P_q co-evolve, guided by X_s and X_q , until a predefined *stopping condition* is met (line 6). This process consists of the following iterative steps: 1) Evaluating the fitness of individuals in both P_s and P_q , updating the archive X with complete solutions and their joint fitness values as determined by the two system versions (line 7); 2) Updating the population archives X_s and X_q based on individual fitness values (lines 8–9); and 3) Breeding new individuals for P_s and P_q , and merging them with X_s and X_q to form the next generation of both populations (lines 10–11). After the *stopping condition* is satisfied, the algorithm returns the final archive X (line 13).

The function *assessFitness* initially computes joint fitness values for complete solutions formed by combining individuals from P_s , P_q , X_s , and X_q . To improve computational efficiency, complete solutions that already exist in X are excluded from re-simulation, avoiding redundant evaluations. After updating the archive X , each individual's fitness value is assigned based on the joint fitness obtained from the complete solutions it contributes to. Finally, fitness clearing is applied to each population to maintain variety within the populations, reducing the risk of premature convergence [67] and the impact of genetic drift [68], which causes the population to converge towards individuals that resemble those with high fitness [69]–[72].

Fig. 1. Overview of *CoCoMagic*.**Algorithm 2:** *assessFitness*

Input: Population of scenarios P_s
 Population of perturbations P_q
 Archive of scenarios X_s
 Archive of perturbations X_q
 Archive of complete solutions X
 Dissimilarity threshold θ
 Execution scenarios \mathbb{S}

Output: Updated population of scenarios P_s
 Updated population of perturbations P_q
 Updated archive of complete solutions X

```

1 Set of complete solutions  $CS \leftarrow \text{collaborate}(P_s, P_q, X_s, X_q);$ 
2 foreach Complete solution  $cs \in CS$  do
3   if  $cs \notin X$  then
4      $\text{execute}(cs);$ 
5      $cs.\text{fitness} \leftarrow \text{Diff}(cs.s, cs.q);$ 
6      $X \leftarrow X \cup \{cs\};$ 
7   end
8 end
9 foreach Population  $P \in \{P_s, P_q\}$  do
10   foreach Individual  $i \in P$  do
11      $i.\text{fitness} \leftarrow \text{assessIndividualFitness}(i, X);$ 
12     if  $\text{Dissim}(i.s, i.q, \mathbb{S}) > \theta$  then
13        $i.\text{fitness} \leftarrow \frac{i.\text{fitness}}{e^{c(\text{Dissim}(i.s, i.q, \mathbb{S}) - \theta)}};$ 
14     end
15   end
16    $\text{fitnessClearing}(P);$ 
17 end
18 return  $P_s, P_q, X;$ 

```

The pseudocode for *assessFitness* is provided in Algorithm 2, with the following inputs: the population of scenarios P_s , the population of perturbations P_q , the population archive of scenarios X_s , the population archive of perturbations X_q , the archive of complete solutions X , the dissimilarity threshold

θ , and the set of execution scenarios \mathbb{S} . The function returns updated populations P_s and P_q with assigned individual fitness values, along with an updated archive X incorporating newly created complete solutions and their corresponding fitness values. The algorithm begins by generating an initial set of complete solutions by combining individuals from both populations and population archives (line 1). Specifically, each individual in P_s collaborates with every individual in X_q , and vice versa for P_q and X_s . For each generated complete solution cs (line 2), if $cs \notin X$, i.e., cs has not been previously evaluated (line 3), it is evaluated by executing both versions of the AS (line 4). The difference in MR violations between the two versions is then quantified using Eq. (2) (line 5), and cs , along with its evaluated result, is added to X (line 6). Upon updating X , the algorithm assigns fitness values to all individuals in both populations. For each population $P \in \{P_s, P_q\}$ (line 9) and for each individual $i \in P$ (line 10), the individual fitness of i is determined as the maximum joint fitness obtained from all complete solutions involving i , calculated according to Eq. (3) (line 11). This strategy of assessing individual fitness using an elitist approach (i.e., choosing the highest fitness value) aligns with findings from previous experimental research [14], [57], [73]. Next, the algorithm applies a penalty to the individual fitness if the dissimilarity between the individual i and the execution scenario set \mathbb{S} , as defined in Eq. (4), exceeds the threshold θ (line 12–13). The penalized fitness is computed as:

$$\text{fitness} := \frac{\text{fitness}_{\text{raw}}}{e^{c(\text{Dissim}(i.s, i.q, \mathbb{S}) - \theta)}}$$

where $\text{fitness}_{\text{raw}}$ denotes the individual fitness value before penalization and c is a constant that controls penalty severity. This exponential decay penalty function [74] ensures that individuals with larger dissimilarity to execution scenarios receive exponentially decreasing fitness values. Finally, the

algorithm performs fitness clearing on each population P (line 16). The algorithm concludes by returning the updated P_s , P_q , and X (line 18).

The function *updatePopulationArchive* updates the population archives X_s and X_q , which play a key role in guiding the search process. Each individual collaborates with archive members to form complete solutions that are evaluated for fitness. Several strategies can be employed to update these archives, such as selecting individuals with the highest fitness values or choosing individuals at random [57]. To balance exploitation and exploration, a hybrid approach may be used, i.e., selecting the top-performing individual along with randomly chosen individuals [57], [62]. This ensures that high-fitness solutions are retained while preserving diversity within the archive, promoting broader exploration of the search space and helping to prevent premature convergence on suboptimal solutions.

The function *breed* generates new individuals by combining selected parents from the current populations. This process drives exploration of the search space and supports the discovery of better solutions over successive generations. It relies on selection, crossover, and mutation operators to produce offspring that inherit characteristics from their parents while introducing variation to maintain diversity. Our algorithm is designed to be flexible, which allows users to define and configure different types of selection, crossover, and mutation operators according to the specific representations of scenarios and perturbations. This user-defined setup ensures adaptability to various ASs and problem contexts, while preserving compatibility with the structure and constraints of the search space.

E. Root Cause Analysis

After generating MR-violating solutions that elicit behavioral differences between two ASs, we introduce an interpretability approach designed to analyze the root causes of these differences in MR violations. Our goal is to uncover the underlying reasons behind the observed behavioral differences, enabling engineers to understand under which conditions the two versions behave differently and how significantly those conditions contribute to the differences. To this end, we extract interpretable rules that describe the behavioral differences between the two versions of an AS. These rules specify, in a human-readable format, the conditions under which differences occur and quantify the extent to which each rule contributes to the observed differences in MR violations. This analysis helps identify potential degradations in the updated AS and enables targeted improvements to enhance system safety, especially by focusing on high-impact conditions.

To extract interpretable rules that explain behavioral differences between two versions of an AS, we employ *RuleFit* [75], a method that generates human-readable rules derived from decision trees trained on input data. According to Margot et al. [76], *RuleFit* is the most accurate algorithm in their evaluation of rule-based algorithms in terms of predictive performance. *RuleFit* operates by first training an ensemble of decision trees and converts each tree's decision paths into

binary rules, where each rule represents a specific combination of feature conditions (e.g., ego vehicle speed $> 70\text{km}/\text{h}$ and weather = foggy). These derived binary rules are then combined with the original features in a sparse linear regression model using Lasso regularization [77]. Lasso helps assign weights to both raw features and derived rules while automatically filtering out less important ones through coefficient shrinkage, improving interpretability and focusing attention on the most relevant patterns.

In our context, we apply *RuleFit* to analyze the differences in MR violations between two versions of an AS by training a model on the generated complete solutions. Each input vector represents a scenario-perturbation pair, i.e., complete solution, incorporating features from both the source scenario and the follow-up scenario created by applying perturbations. These features typically include continuous and categorical variables, such as ego vehicle initial speed, object positions, and environmental conditions relevant to testing ADSSs. To ensure compatibility with *RuleFit*, preprocessing such as one-hot encoding is often required for categorical features, converting them into binary indicators that the model can process alongside continuous variables. The target variable is the observed difference in MR violations between the two system versions for each complete solution. In the end, the *RuleFit* model outputs a set of human-readable IF-clause rules along with coefficients and support values for the original and derived features. Each rule's coefficient quantifies its contribution to predicting the difference in MR violations, while the support value indicates the proportion of complete solutions where the rule's conditions hold.

By examining these rules, we can identify scenario patterns that most strongly influence behavioral differences between the two versions. For example, a rule such as “IF ego vehicle speed $> 70\text{km}/\text{h}$ AND foggy weather = true, THEN the difference in MR violation increases by 2.5” suggests that under high-speed, foggy conditions, the two system versions behave more inconsistently, with the updated system likely exhibiting a higher MR violation. Such insights help developers and testers focus their efforts by highlighting specific scenario conditions where updates may have introduced unintended behaviors or safety risks. These interpretable rules directly support both root cause analysis and actionable decision-making, such as prioritizing which scenario types to investigate further or monitor more closely in future system updates.

V. EMPIRICAL EVALUATION

In this section, we empirically evaluate the effectiveness and efficiency of *CoCoMagic* in generating test cases that reveal differences in MR violations between two versions of the AS under test, comparing our approach against two baseline methods. We further investigate how the use of constraints and population initialization strategies influences the similarity between the identified test cases and the collected execution scenarios that represent the real-world operating conditions. Finally, we assess how our interpretability approach contributes to capturing the underlying root causes of the observed differences in MR violations between the two ASs

under test. Specifically, we answer the following Research Questions (RQs).

RQ1: How effectively can *CoCoMagic* find test cases revealing differences in MR violations compared to baseline methods?

To answer RQ1, we evaluate the performance of different search methods in terms of the number of distinct complete solutions identified that reveal the differences in violations of predefined MRs within a given search budget.

RQ2: How efficiently can *CoCoMagic* find test cases revealing differences in MR violations compared to baseline methods?

To answer RQ2, we examine the speed at which different search methods identify distinct complete solutions that reveal the differences in violations of predefined MRs.

RQ3: To what extent do the applied constraints and population initialization strategies affect the similarity of identified test cases to execution scenarios?

To answer RQ3, we analyze the impact of constraints and population initialization strategies. First, we evaluate how these factors influence the similarity of the identified complete solutions to the execution scenarios. Next, we assess their effect on the overall effectiveness of the search process. Understanding these aspects is essential to determine whether our approach effectively guides the search toward more realistic solutions and to identify any potential negative side effects.

RQ4: To what extent does our interpretability approach contribute to identifying the root causes of the differences in MR violations?

To answer RQ4, we examine the accuracy and support of interpretable rules, extracted from the identified complete solutions, in explaining the observed differences in MR violations.

A. Baseline Methods

Since our work is the first to systematically generate test cases aimed at revealing differences in MR violations between two versions of an AS, there are no existing methods tailored for this exact problem. To enable meaningful comparison, we evaluate *CoCoMagic* against two baseline strategies that reflect commonly used search paradigms in test generation.

- **Random Search (RS):** This baseline involves generating test cases through uniform random sampling without any guidance from fitness feedback. Although simple, *RS* provides a useful reference point to assess the inherent difficulty of the search and the value of guided optimization.
- **Standard Genetic Algorithm (SGA):** This variant applies a standard genetic algorithm [78] using a single population, treating the entire solution space as a uniform search domain. Unlike our method, it does not differentiate between scenario structure and perturbation behaviors. Comparing with *SGA* helps highlight the benefits of our cooperative co-evolutionary setup.

By including these two baselines, we aim to illustrate both the relative performance gains achieved through guided search and the contribution of our modular co-evolutionary design to the quality and diversity of the generated test cases.

B. Experimental Setup

This subsection outlines the setup used to evaluate the RQs, including details about the simulation environment, the collected execution scenarios, the MRs employed, and the parameter configurations for both *CoCoMagic* and the baseline methods.

1) *Simulation Environment:* Our experiments were conducted using CARLA [79], a widely used open-source simulator tailored for autonomous driving research. CARLA enables the creation of complex, interactive driving scenarios featuring configurable weather, traffic, and environmental elements. To ensure realistic perception and behavior, we incorporated INTERFUSER [13], a state-of-the-art multi-modal end-to-end ADS that ranks among the top performers on the official CARLA *Leaderboard* [35]. INTERFUSER fuses data from LiDAR and Camera sensors to deliver reach scene information.

Experiments were executed on a dedicated high-performance server equipped with 56 CPU cores and 2 GPUs (each with 48GB of memory). To increase throughput, we deployed 6 parallel CARLA instances in separate Docker containers, leveraging CUDA 12.4 for GPU-accelerated computation. This setup enabled concurrent scenario evaluations at scale using CARLA version 0.9.10.1.

2) *Execution Scenarios:* We collected a diverse set of execution scenarios by running INTERFUSER in CARLA *Leaderboard* environments, across four different towns and eight distinct weather conditions, including clear skies, medium rain, and heavy rain under varying lighting conditions, e.g., noon and sunset. The CARLA *Leaderboard evaluator* is a standardized evaluation framework that runs INTERFUSER through a variety of driving tasks in simulated urban environments, enabling consistent and reproducible assessment of driving performance.

To ensure temporal and spatial diversity, we sampled execution data (including static and dynamic parameters of the environment) at fixed time intervals (every 5 seconds) following a random offset from the beginning of each route execution. This approach allowed us to capture a variety of driving states without over-representing any particular region or weather condition. We limited the number of sampled scenarios per route-weather configuration to encourage balanced coverage, resulting in approximately 800 distinct execution scenarios used for our experiments.

3) *Metamorphic Relations:* We used a set of 11 MRs from Table I, drawn from established research [60], [80], [81], selected based on their compatibility with both the ADS under test and the simulation platform. Some MRs from prior literature were excluded due to incompatibility with the constraints of our simulator.

To facilitate evaluation, we grouped the MRs into two categories, i.e., GP_1 and GP_2 , based on their output behavior. GP_1 includes MRs with expected speed reductions in response to environmental or traffic changes. GP_2 captures invariance-based relations, i.e., changes in actors should not significantly alter the vehicle's steering behavior.

In the following subsections, we report the results for GP_1 . The outcomes for GP_2 are consistent with those of GP_1 , thereby demonstrating the robustness of *CoCoMagic* across different

TABLE I
MRs INVOLVED IN THE EXPERIMENTS.

Category	MR	Description
<i>GP₁</i> Speed Reduction	<i>MR₁</i> [*]	If a pedestrian appears on the roadside, then the ego vehicle should slow down.
	<i>MR₂</i> ^{*,†}	If the driving time changes into night, then the ego vehicle should slow down.
	<i>MR₃</i> [†]	Adding a vehicle in the front of the ego vehicle, the speed of the ego vehicle should decrease.
	<i>MR₄</i> [†]	Adding a pedestrian in the front of the ego vehicle, the speed of the ego vehicle should decrease.
	<i>MR₅</i> [†]	Changing from sunny to rainy, the speed of the ego vehicle should decrease.
<i>GP₂</i> Actor Invariance	<i>MR₆</i> [‡]	In a given driving scenario where the ego vehicle detects a target obstacle and attempts to avoid a collision, the ego vehicle should keep the steering unchanged when the speed of the ego vehicle changes (increased or decreased by a certain factor).
	<i>MR₇</i> [‡]	In a given driving scenario where the ego vehicle detects a target obstacle and attempts to avoid a collision, the ego vehicle should keep the steering unchanged the same when adjusting (i.e., scaled down or up) the size of the ego vehicle.
	<i>MR₈</i> [‡]	In a given driving scenario where the ego vehicle detects a target obstacle and attempts to avoid a collision, the ego vehicle should keep the steering unchanged when adjusting (i.e., scaled down or up) the size of the target obstacle.
	<i>MR₉</i> [‡]	In a given driving scenario where the ego vehicle detects a target obstacle and attempts to avoid a collision, the ego vehicle should keep the steering unchanged when changing the position of the ego vehicle.
	<i>MR₁₀</i> [‡]	In a given driving scenario where the ego vehicle detects a target obstacle and attempts to avoid a collision, the ego vehicle should keep the steering unchanged when changing the speed of the target obstacle.
	<i>MR₁₁</i> [‡]	In a given driving scenario where the ego vehicle detects a target obstacle and attempts to avoid a collision, the ego vehicle should keep the steering unchanged when adding additional actors.

* These MRs are derived from study [60].

† These MRs are derived from study [80].

‡ These MRs are derived from study [81].

MR groups. To avoid redundancy, the detailed results for *GP₂*, including all supporting figures, are presented in the appendix.

4) *Parameter Settings*: All methods were executed with a simulation budget of 200, chosen based on pilot experiments that demonstrated sufficient convergence behavior under this limit. To ensure fair comparisons, each method was allowed to use up to 200 scenario evaluations.

We configured each method to use a population of 5 individuals, balancing between computational cost and search effectiveness. Given the high cost of each fitness evaluation (approximately two minutes per test case), this smaller population size aligns with common practice in search-based testing literature [82], [83]. For both *CoCoMagic* and *SGA*, we adopted tournament selection with a size of 3, which strikes a good balance between exploration and exploitation [84]–[86]. This choice also helps avoid premature convergence, especially in small populations. We set the mutation and crossover rates to 0.2 and 0.8, respectively, consistent with recommendations in the evolutionary computation literature [87], [88]. As for *CoCoMagic*, which relies on cooperative co-evolution, we tuned its specific hyperparameters via lightweight exploratory runs. The final settings included an archive size of 3 per population, with crossover and mutation rates mirroring those used in *SGA*.

Due to the nature of population-based algorithms, some methods may slightly exceed the 200-simulation budget per run, since evaluations occur in batches. In such cases, the

actual number of simulations consumed per generation can vary between methods, leading to misalignment in budget usage. To ensure consistent comparisons, we applied linear interpolation on all evaluation metrics at points where the actual simulations deviated from the predefined budget. This process estimates metric values precisely at the intended search budgets by interpolating between the closest available points, enabling a fair assessment under an aligned computational budget.

C. RQ1: Effectiveness of *CoCoMagic*

1) *Methodology*: To answer RQ1, we evaluate the effectiveness of *CoCoMagic* in identifying test cases, i.e., complete solutions, that amplify behavioral differences between two versions of INTERFUSER. Unlike existing MR approaches that target outright violations of predefined properties, our objective is to identify solutions that exhibit large discrepancies in their effects on the two ADS versions. We compare *CoCoMagic* against the two baseline methods under the same search budget, using the ***Distinct Solutions (DS)*** metric as the primary indicator of effectiveness.

DS denotes the number of distinct complete solutions that expose significant behavioral differences between the ADS versions. We require such solutions to satisfy the following conditions: 1) its fitness value, i.e., the measured difference in MR violations across ADS versions, exceeds a predefined fitness threshold θ_f , and 2) it is sufficiently different from other selected solutions based on a minimum distance threshold θ_d . Formally, let CS_V be the set of complete solutions identified by method *V* that satisfy the above criteria. The number of distinct solutions is defined as $DS(V) := |CS_V|$.

To ensure a comprehensive evaluation, we assess each method under multiple configurations of the fitness threshold θ_f and distance threshold θ_d . The fitness threshold controls the required degree of behavioral difference between the two ADSs, reflecting the severity of the identified complete solutions, where higher values correspond to more substantial differences. The distance threshold, on the other hand, governs the minimal dissimilarity between retained solutions, thus controlling the diversity of the complete solutions. By exploring a wide range of threshold values, we are able to compare the performance of different approaches under varying demands for severity and diversity of the generated complete solutions. Specifically, we use $\theta_f \in \{0.5, 0.8, 1.0, 1.3, 1.5, 2.0\}$ to cover a meaningful spectrum of behavioral differences observed across all methods. This range was chosen to approximately extend up to the 70th percentile of the fitness values observed in our experiments (around 2.0), ensuring that the selected thresholds capture realistic and informative levels of severity. Solutions with fitness below 0.5 are excluded due to their limited discriminative value and minimal impact on differentiating between the two ADSs. For θ_d , we consider values from 0.0 to 4.0 in increments of 0.4, covering a range of diversity requirements from lenient to stringent. The upper bound was selected based on the 95th percentile of pairwise distances among all generated solutions, ensuring that the threshold range meaningfully reflects the observed distribution of solution diversity.

To complement the *DS* metric, we also assess the quality of solutions generated by each method based on their fitness

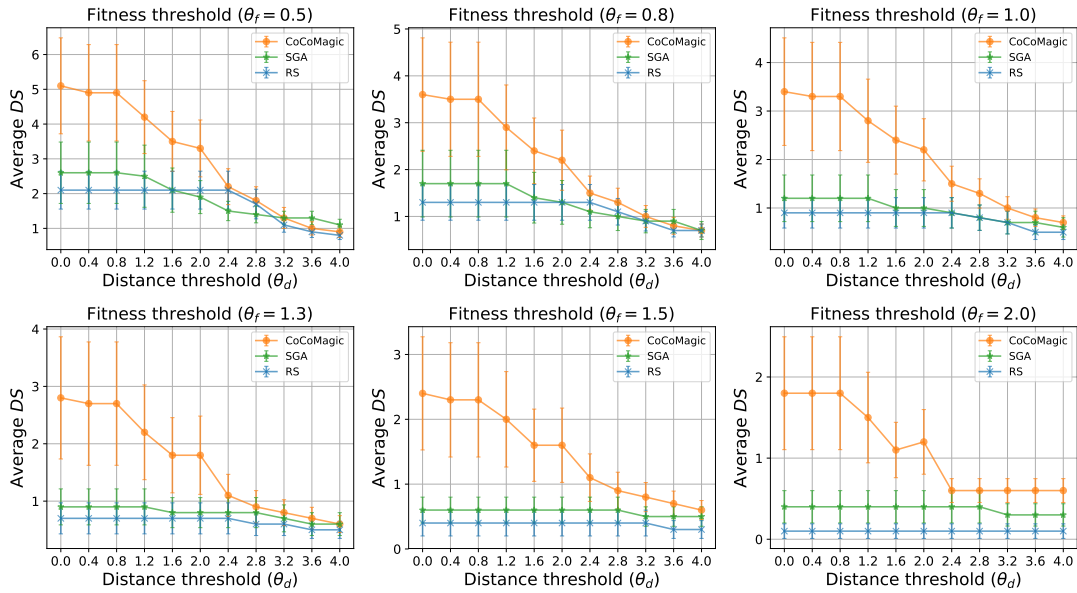


Fig. 2. *Distinct Solutions (DS)* vs. distance threshold (θ_d) across different fitness thresholds (θ_f). A higher *DS* value indicates more distinct test cases discovered by the method. Each curve plots the average *DS* value at different θ_d settings, under a specific fitness threshold θ_f . This figure reveals how each method balances the quantity and diversity of test cases as θ_f varies.

values. Specifically, we analyze the distribution of fitness values across all complete solutions produced by each approach, where a higher fitness indicates greater differences in MR violations. This provides insight into each method's capacity to uncover critical test cases that induce pronounced behavioral differences between the two ADSs.

2) *Results*: Fig. 2 reports the average *DS* values across 10 distinct experiments, achieved by *CoCoMagic*, *SGA*, and *RS*, at varying θ_d and θ_f . Each subplot shows the average *DS* values over executions, as a function of θ_d , with 95% confidence intervals represented by error bars. Different subplots correspond to different fitness thresholds θ_f .

Across almost all settings, *CoCoMagic* consistently outperforms both *SGA* and *RS* in terms of discovering a greater number of distinct complete solutions that highlight behavioral differences between ADS versions. Notably, under stricter fitness thresholds ($\theta_f \geq 1.0$), *CoCoMagic* surpasses the baseline methods across all distance thresholds, demonstrating its strong capability in uncovering solutions that reveal large behavioral differences between the two ADSs. For moderate fitness and distance thresholds ($\theta_f = 1.0, \theta_d = 2.0$), *CoCoMagic* identifies an average of 2.2 distinct solutions within the specified budget, outperforming *SGA* and *RS*, which yield only 1.0 and 0.9 distinct solutions, respectively. On average, *CoCoMagic* discovers 108% ($p\text{-value} < 10^{-5}$) more distinct solutions than *SGA* and 287% ($p\text{-value} < 10^{-13}$) more than *RS*, underscoring its effectiveness in uncovering behavioral differences between the two ADS versions. To assess the statistical significance of these differences, we conducted non-parametric Mann-Whitney U tests with Fisher's method for p -value correction [89].

Varying the fitness threshold θ_f reveals how each method adapts to increasing demands for the severity of behavioral differences in the generated solutions. As θ_f increases from

0.5 to 2.0, *DS* naturally decreases across all methods, since fewer solutions exhibit large enough behavioral differences to surpass stricter fitness criteria. Nonetheless, *CoCoMagic* consistently maintains a clear lead over both *SGA* and *RS* at every fitness threshold, indicating its robustness in discovering complete solutions even under stringent thresholds. This advantage is particularly evident at higher fitness thresholds ($\theta_f \in \{1.5, 2.0\}$), where *CoCoMagic* continues to discover more solutions than both *SGA* and *RS*, who struggle to identify hardly any high-fitness solutions. As the distance threshold θ_d increases, all methods show a reduction in *DS* values, which is expected since stricter diversity requirements lead to the exclusion of more solutions, and thereby reduce the number of retained complete solutions. Nevertheless, *CoCoMagic* retains a significant advantage across nearly all θ_d settings. These results demonstrate that our approach is more effective in navigating the search space and detecting solutions exhibiting high behavioral discrepancies between system versions.

In addition to the *DS* metric, we evaluate the quality of complete solutions produced by each method, excluding those with insignificant fitness values (< 0.1). This thresholding serves as a post-processing step to filter out solutions with near-zero fitness, which typically arise from randomness in the process and do not reflect genuine differences in violations. The filtering ensures that the comparison focuses only on meaningful solutions of practical relevance. Fig. 3 presents the distribution of average fitness of complete solutions generated by *CoCoMagic*, *SGA*, and *RS* across 10 independent executions. *CoCoMagic* achieves both higher median and mean fitness values compared to the baselines, indicating a greater capacity to uncover solutions that induce stronger behavioral discrepancies between the two system versions. On average, solutions generated by *CoCoMagic* reach a fitness value of

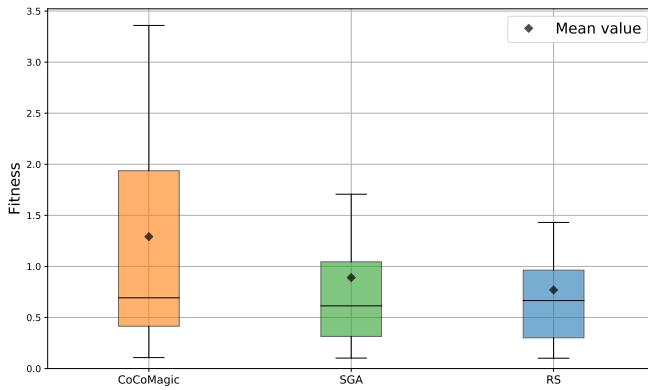


Fig. 3. Fitness distribution of test cases generated by *CoCoMagic*, *SGA*, and *RS*. Higher fitness indicates that the discovered test cases induce greater differences in the violations exhibited by the two ADSs. Each box shows the fitness values of the test cases across 10 executions, providing insight into the peak effectiveness of each method. This figure highlights the relative strength of each method in uncovering critical test cases with severe behavioral differences.

1.29, representing a 45% (p -value ≈ 0.0349) increase over *SGA* (0.89) and a 68% (p -value ≈ 0.0351) increase over *RS* (0.77).

In addition to the higher median and mean fitness, Fig. 3 highlights that *CoCoMagic* also attains a substantially larger range of fitness values compared to the baselines. While *SGA* and *RS* peak at fitness levels around 1.70 and 1.43, respectively, *CoCoMagic* reaches up to 3.35. This indicates that *CoCoMagic* not only consistently yields stronger solutions on average but is also capable of uncovering more severe cases that trigger significantly larger behavioral differences between the two system versions.

In summary, the results clearly demonstrate the superior effectiveness of *CoCoMagic* compared to both baseline methods in identifying a greater number of distinct test cases that not only satisfy diversity requirements but also induce more severe behavioral discrepancies between the two ADS versions. Its ability to generate both critical and diverse test cases highlights the strength of its co-evolutionary search strategy in navigating complex search spaces and uncovering meaningful discrepancies, making it an effective framework for rigorous differential testing of ASs.

Answer to RQ1

CoCoMagic outperforms *SGA* by 108% and *RS* by 287% in detecting severe differences in MR violations, as measured by the average *DS* metric. In addition, it achieves an average fitness that is 45% higher than *SGA* and 68% higher than *RS*, underscoring its effectiveness in uncovering more pronounced behavioral discrepancies.

D. RQ2: Efficiency of *CoCoMagic*

1) *Methodology*: To address RQ2, we analyze the rate at which different methods discover complete solutions over the course of their search. To this end, we track the number of

distinct solutions identified by each method as a function of the search budget, expressed as a percentage of the total number of simulations allowed. The methodology follows that of RQ1, employing the same hyperparameters and repeating each method 10 times. The only difference is that the search budget is increased from 200 to 500 simulations. This larger budget provides a much stronger basis for evaluating the algorithms' efficiency over extended runs, yielding more reliable insights into their efficiency over time. The drawback, however, is that it significantly increases execution time, which can limit practicality in fast-paced development settings where quick feedback is essential.

The resulting plots depict *DS* versus the search budget, where each curve reflects how quickly a method accumulates unique test cases that reveal differences in MR violations under varying fitness thresholds θ_f and distance thresholds θ_d . To support a quantitative comparison across methods and settings, we compute the *Area Under the Curve (AUC)* for each *DS*-budget curve. The *AUC* serves as an aggregate measure of efficiency, where higher values indicate that a method finds more distinct solutions earlier during the search. This metric is particularly suitable for our setting, as it captures both the speed and volume of distinct solutions discovered, which are two central factors in assessing the efficiency of test generation. It allows us to compare algorithms not only at final budget levels but throughout the entire simulation horizon.

In addition to the *DS*-budget analysis, we assess the computational efficiency of the algorithms in terms of execution time. For each method, we record the wall-clock time required to complete the search budget across 10 runs. This metric provides complementary insights, highlighting differences in computational cost of running the algorithms and offering a practical perspective on their suitability for cost-sensitive testing scenarios.

2) *Results*: Fig. 4 presents the average *DS* values over simulation budget for each method, under nine different configurations of fitness thresholds θ_f and distance thresholds θ_d . Each subplot corresponds to a specific threshold setting, capturing lenient ($\theta_f = 0.5$), moderate ($\theta_f = 1.5$), and high ($\theta_f = 2.5$) severity requirements, each paired with increasing levels of diversity ($\theta_d = 1.0, 1.6, 2.3$). The distance thresholds were selected based on their filtering effect on the generated solutions. On average, $\theta_d = 1.0, 1.6$, and 2.3 remove about 10%, 30%, and 50% of the solutions produced by all methods. These values, therefore, correspond to low, moderate, and high diversity constraints.

Across nearly all configurations, *CoCoMagic* consistently outperforms the baseline methods in the total number of distinct solutions discovered over time. Moreover, *CoCoMagic* maintains a steady and steeper growth trajectory compared to the baselines, which reflects the advantage of the co-evolutionary setting in promoting the discovery of additional distinct solutions as the budget increases. As the fitness threshold becomes stricter ($\theta_f \in \{1.5, 2.5\}$), the number of retained solutions decreases for all methods, leading to lower overall *DS* values. Nevertheless, *CoCoMagic* maintains a clear advantage over the others. For example, under thresholds $\theta_f = 1.5$ and $\theta_d = 1.6$, *CoCoMagic* nearly doubles the number

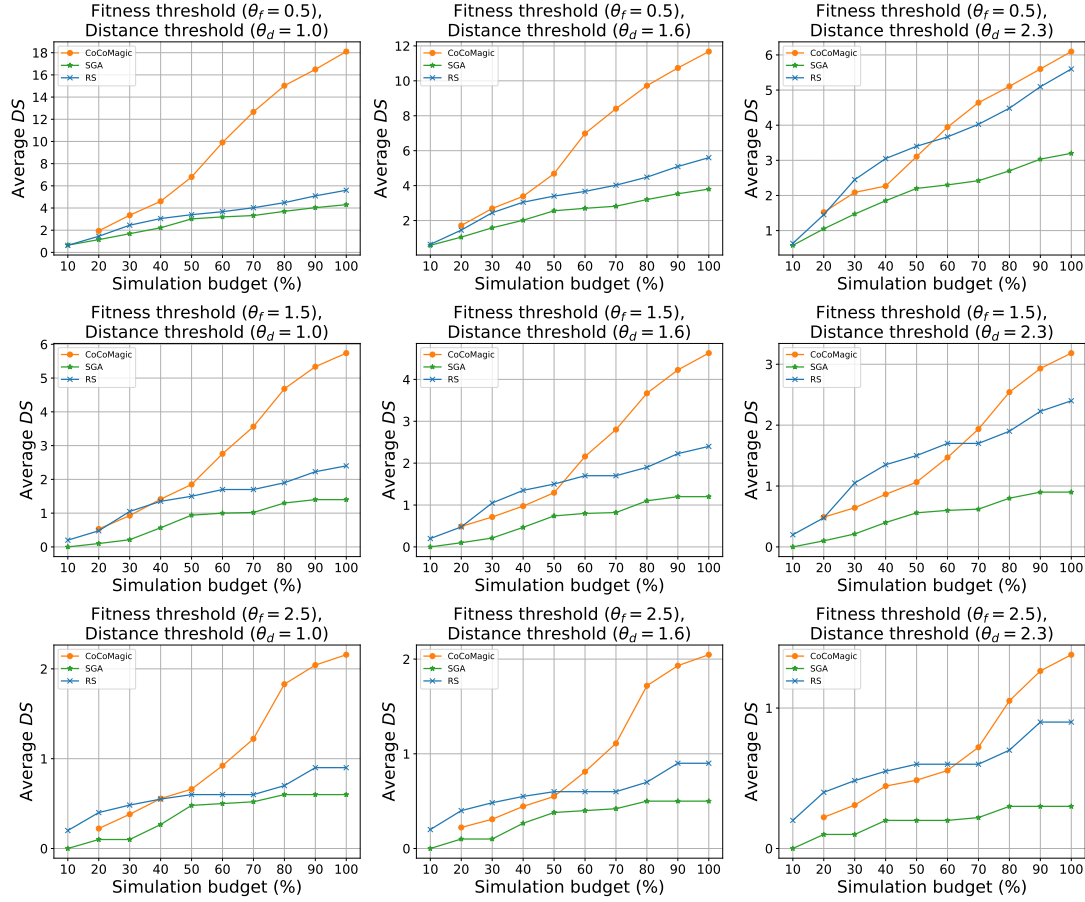


Fig. 4. *Distinct Solutions (DS)* progression across simulation budget levels. Each subplot illustrates how the *DS* value grows as more simulation resources are consumed, under specific combinations of fitness thresholds (θ_f) and distance thresholds (θ_d). The curves represent different methods, allowing a direct comparison of how quickly and effectively each approach uncovers severe and diverse behavioral discrepancies between ADS versions. Sharper increases and higher endpoints indicate greater efficiency in identifying test cases early in the search process.

of discovered distinct solutions relative to *RS* and four times the *DS* values compared to *SGA* by the 100% budget mark. Under higher diversity restrictions $\theta_d = 2.3$, *RS* starts to perform competitively, specifically at early stages of the search process (budget $< 60\%$). This demonstrates the advantage of random exploration in generating a diverse set of solutions when constraints are stringent. However, as the budget grows (budget $\geq 70\%$), *CoCoMagic* surpasses *RS* in *DS* values, illustrating the advantage of systematic search and diversity optimization over pure exploration, in sustaining progress and uncovering more solutions over extended runs.

To quantitatively assess the overall efficiency of each method, we compute the *AUC* for the *DS*-budget curves shown in Fig. 4. This metric aggregates the progression of distinct solution discovery over the entire simulation budget, offering a single representative value for each configuration. A higher *AUC* indicates that a method finds more distinct solutions earlier and more consistently throughout the search process. On average, *CoCoMagic* outperforms *SGA* by 184% and *RS* by 54% in terms of *AUC*, demonstrating more efficient test case generation under budget constraints. Statistical analysis using the Wilcoxon signed-rank test [90] confirms the significance of these improvements, with $p\text{-value} < 10^{-2}$ against both

baselines.

In addition to evaluating the discovery rate of distinct solutions over budget, we also examined the computational efficiency of the algorithms. Fig. 5 presents the distribution of execution times (in hours) across 10 runs for *CoCoMagic*, *SGA*, and *RS*. The results show that *CoCoMagic* consistently requires less computational time, with an average of 7.24 hours, compared to 10.48 hours for *SGA* and 8.74 hours for *RS*. This indicates that our approach is not only more effective in utilizing the search budget but also faster in execution. Specifically, *CoCoMagic* improves average execution time by 30.97% over *SGA* ($p\text{-value} < 10^{-3}$) and by 17.21% over *RS* ($p\text{-value} < 10^{-3}$).

Overall, these results demonstrate that *CoCoMagic* is significantly more budget-efficient in discovering critical and diverse test cases, while also achieving faster execution compared to the baselines. These advantages make *CoCoMagic* better suited for cost-sensitive testing scenarios.

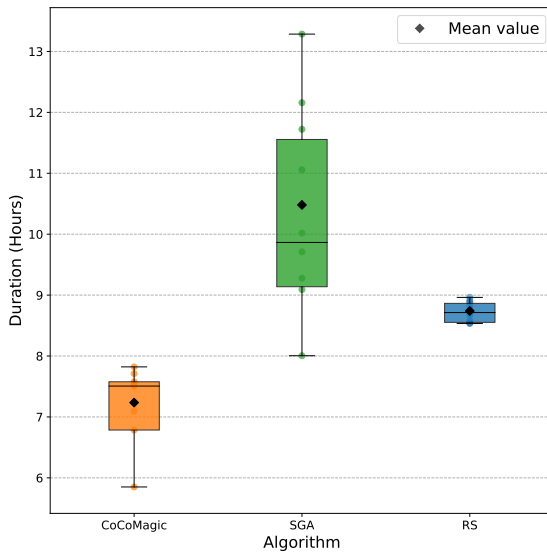


Fig. 5. Distribution of execution times (in hours) for *CoCoMagic*, *SGA*, and *RS* under a fixed search budget. Lower execution time indicates greater computational efficiency in completing the search. Each box summarizes the distribution of execution times across 10 runs.

Answer to RQ2

CoCoMagic outperforms *SGA* by 184% and *RS* by 54% in terms of overall efficiency, as measured by the *AUC* of the *DS*-budget curves, demonstrating its superior ability to discover critical and diverse test cases within a limited search budget. In addition, it achieves a 31% faster execution time compared to *SGA* and 17% faster than *RS*, confirming its advantage in computational efficiency.

E. RQ3: Impact of Constraints and Population Initialization

1) *Methodology*: To investigate the impact of constraining mechanisms and population initialization strategies on the effectiveness of *CoCoMagic*, we designed a set of experiments involving different configurations of *CoCoMagic*. The first configuration represents the standard constrained version, where the search is forced to remain within a specified similarity to recorded execution scenarios. In the second configuration, denoted as *CoCoMagic*\c, the constraint was removed to assess its influence on the quantity and quality of generated test cases. To evaluate the effect of the initialization strategy, we introduced an alternative method termed *Runtime Initialization* (*RI*), where the initial population is sampled directly from the previously collected execution scenarios, rather than being generated randomly. We applied this initialization strategy to both the constrained and unconstrained variants, resulting in a total of four experimental configurations.

Each configuration was executed independently 10 times to account for stochastic variation in the search process. For all runs, we employed the same effectiveness metrics as in RQ1: 1) the *DS* metric, capturing the number of generated distinct solutions, and 2) the average fitness of the test cases found by each configuration, quantifying the capacity of uncovering

critical test cases with severe behavioral discrepancies. In addition, we report the *Average Execution Distance* (*AED*), which measures how closely the generated test cases resemble real-world execution scenarios. For each test case, we compute its distance to the nearest execution scenario (see Eq. (4)) and then aggregate these values by averaging over all test cases in a given run. This metric provides insights into how well the generated scenarios align with observed real-world scenarios.

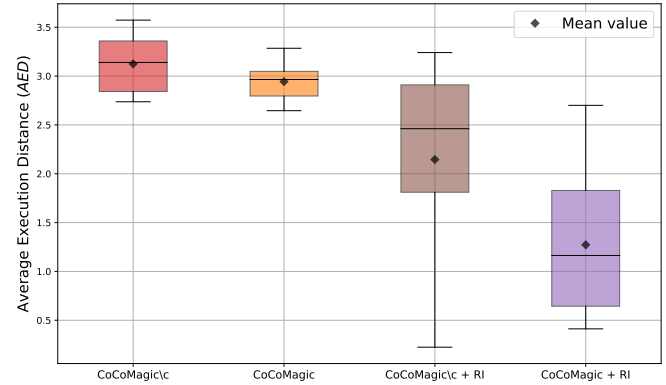


Fig. 6. *Average Execution Distance* (*AED*) between identified test cases and execution scenarios under different configurations of *CoCoMagic* and baseline methods. Higher *AED* values indicate that the generated test cases are more distinct from the execution scenarios. Each box summarizes the distribution of *AED* values for a given method, highlighting how closely the identified test cases resemble previously observed real-world scenarios.

2) *Results*: Fig. 6 shows the *AED* between the generated complete solutions and the set of previously observed execution scenarios. This metric reflects how closely the identified solutions resemble behaviors observed during actual system executions. Lower *AED* values indicate that the generated complete solutions are behaviorally closer to known execution scenarios, whereas higher values suggest the discovery of more dissimilar solutions.

The most noticeable trend in Fig. 6 is the substantial reduction in *AED* values achieved by both *RI* configurations. *CoCoMagic* with *RI* produces the lowest *AED* values overall, followed by its unconstrained counterpart. This outcome confirms the effectiveness of *RI* in guiding the search toward solutions that remain close to observed ones. By seeding the population with scenarios observed during actual executions, *RI* biases the search toward regions of the search space that are more contextually grounded. In contrast, the unconstrained and constrained configurations without *RI* (i.e., *CoCoMagic*\c and *CoCoMagic*) yield significantly higher *AED* values, with distributions clustered around a much higher median. This confirms that, in the absence of *RI*, the search is more likely to generate complete solutions that deviate from what is commonly observed, resulting in less realistic but potentially more severe solutions.

The impact of the constraining mechanism is particularly evident when comparing constrained and unconstrained variants within each initialization strategy. In both cases, applying the constraint leads to lower *AED* values, indicating that the constraint effectively guides the search toward solutions that are closer to the observed execution scenarios. Quantitatively, apply-

ing the constraint alone yields a modest improvement of 5.87% in average *AED* value (2.94) compared to its unconstrained counterpart (3.13). The benefit becomes more pronounced when *RI* is introduced. The unconstrained variant with *RI* reduces the average *AED* value by 31.38% (2.15) relative to the non-*RI* variant. When combining both *RI* and constraining, the search is tightly focused around the execution scenarios, resulting in the most significant improvement of 59.31% (1.27) reduction in *AED*. This highlights the complementary role of constraints in enhancing behavioral realism, especially when the initial population is already grounded in the observed execution scenarios. Overall, these results underscore the effectiveness of both *RI* and the constraining mechanism in promoting the realism of generated test cases.

Fig. 7 compares the average number of distinct solutions discovered by each configuration of *CoCoMagic*, across varying distance thresholds (θ_d) and fitness thresholds (θ_f). Across all settings, it is apparent that removing the constraint (*CoCoMagic\c*) consistently yields a higher average *DS* value compared to the constrained version (*CoCoMagic*). This suggests that unconstrained search allows the algorithm to explore a broader portion of the search space, improving its ability to uncover diverse solutions.

Introducing *RI* leads to a noticeable reduction in *DS* values, for both constrained and unconstrained variants. This reduction can be attributed to the tighter focus imposed by sampling initial populations from execution scenarios, which biases the search toward more realistic, but potentially more restricted regions of the search space. However, *RI* exhibits reduced sensitivity to the distance threshold θ_d ; both *RI* variants maintain a more stable *DS* value compared to their counterparts, as θ_d increases. This robustness is likely due to the higher diversity inherent in the sampled execution scenarios used for initialization, which enables the generation of complete solutions that are already dispersed across different behavioral regions.

These trends are also reflected quantitatively in the overall reduction of *DS* values compared to the unconstrained, non-*RI* baseline (*CoCoMagic\c*). Applying the constraint alone results in a 21.67% (*p*-value $< 10^{-2}$) decrease in the *DS* metric, highlighting the limiting effect of realism enforcement on exploratory diversity. Introducing *RI* to the unconstrained variant leads to a slightly larger reduction of 23.74% (*p*-value $< 10^{-7}$), while combining both constraints and *RI* produces the most substantial drop, with a 39.19% (*p*-value $< 10^{-11}$) decrease in *DS*. These results confirm the previously discussed trade-off: while constraints and *RI* improve behavioral realism, they reduce the algorithm's ability to discover a wide range of distinct solutions.

Interestingly, under lower fitness thresholds, the *RI* variants begin to outperform their non-*RI* counterparts at higher values of θ_d . For example, when $\theta_f \in \{0.5, 0.8\}$ and $\theta_d \geq 3.2$, both *RI* configurations yield more solutions than their counterparts. This is likely explained by the inherent diversity of the execution scenarios, which is carried over to the initial population through direct sampling. Such initialization helps sustain diversity when the diversity requirement (via θ_d) is high and fitness constraints are relatively loose. However, as fitness thresholds increase ($\theta_f \geq 1.0$), the *RI* variants fall behind, indicating that although

RI supports early diversity, it may hinder the discovery of highly critical solutions, as it limits the algorithm's ability to detect severe edge-cases that are not represented in the selected execution scenarios.

Fig. 8 presents the fitness distribution of solutions identified by each configuration, excluding those with insignificant fitness values (< 0.1), across 10 executions. The metric reflects the severity of the discovered solutions, with higher values indicating more critical discrepancies between the two ADS versions.

As shown in Fig. 8, the unconstrained variant (*CoCoMagic\c*) achieves the highest average fitness across runs, followed closely by the constrained variant. This observation may suggest that removing the constraint allows the search to better exploit regions of the search space that lead to more severe discrepancies. However, the small reduction in average fitness observed for *CoCoMagic* and *CoCoMagic\c+RI* relative to *CoCoMagic\c* is not statistically significant, suggesting that there is no solid evidence that introducing constraints or initialization with execution scenarios diminishes the ability to find severe discrepancies. In contrast, the reduction observed for *CoCoMagic+RI* compared to *CoCoMagic\c* is statistically significant. This indicates that when both constraints and initialization are applied together, the search is more strongly biased toward typical or nominal driving patterns, which restricts access to the rare edge-case behaviors that produce higher-fitness solutions.

Quantitative comparisons provide insights into the effect of constraints and *RI* on the severity of discovered solutions. Applying the constraint alone leads to a reduction of 14.08% in average fitness values, with the constrained configuration (*CoCoMagic*) achieving an average fitness of 1.29 compared to 1.50 for the unconstrained baseline (*CoCoMagic\c*). Similarly, incorporating *RI* into the unconstrained variant yields a 21.09% decrease, with an average fitness of 1.19. However, neither of these reductions is statistically significant ($p \approx 0.08$ and $p \approx 0.1$, respectively). In contrast, combining both constraints and *RI* produces a substantial and statistically significant reduction, with an average fitness of 0.75, corresponding to a 49.93% drop from the baseline ($p < 10^{-4}$).

Overall, these findings indicate that applying either constraints or *RI* alone can slightly reduce the severity of the generated solutions by limiting exploration. Yet, this effect is negligible and statistically insignificant. In contrast, combining the two introduces a significant reduction in severity, demonstrating that their joint influence can substantially restrict the search from reaching highly critical discrepancies.

In summary, the results of RQ3 reveal a clear trade-off between behavioral realism and exploratory power when applying constraints and *RI*. While both mechanisms independently and jointly reduce the number and severity of generated test cases, they significantly enhance alignment with real-world scenarios, as evidenced by lower *AED* values. *RI* proves especially effective in grounding the search, but it also significantly restricts access to edge-case solutions, particularly under stricter fitness requirements. Conversely, unconstrained and randomly initialized search enables broader exploration and uncovers more critical solutions, though at the cost of lower realism.

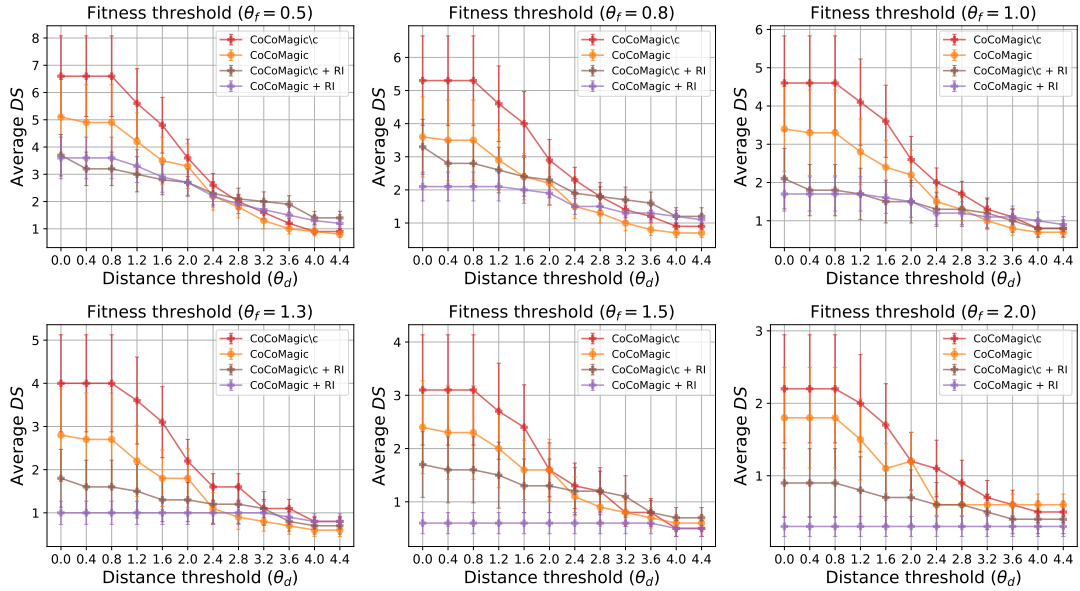


Fig. 7. *Distinct Solutions (DS)* vs. distance threshold (θ_d) across different fitness thresholds (θ_f) for different configurations of *CoCoMagic*. A higher *DS* value indicates more distinct test cases discovered by the method. Each curve plots the average *DS* value at different θ_d settings, under a specific fitness threshold θ_f . This figure reveals how each method balances the quantity and diversity of test cases as θ_f varies.

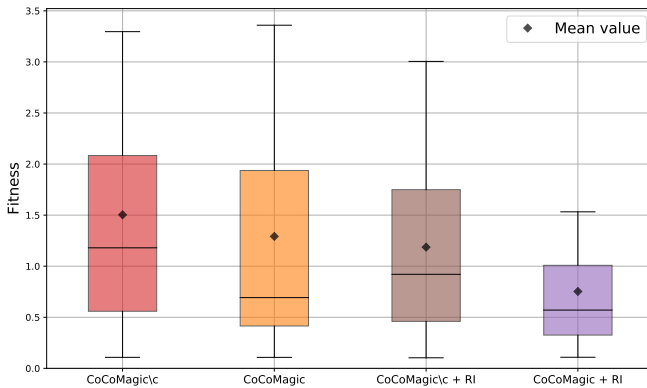


Fig. 8. Average fitness of test cases generated by different configurations of *CoCoMagic*. Higher average fitness indicates that the discovered test cases induce greater differences in the violations exhibited by the two ADSs. Each box shows the average fitness values of the generated test cases across 10 executions. This figure highlights the relative strength of each method in uncovering test cases with severe behavioral differences.

Answer to RQ3

Both constraints and *RI* improve the behavioral realism of generated test cases, as measured by *AED*, with their combination yielding around 50% improvement over the unconstrained baseline. However, these mechanisms also tend to reduce the number of discovered solutions. The constraint alone leads to a 22% reduction in *DS* values. Incorporating *RI* further decreases *DS* values by up to 39%. This reveals a clear trade-off in which constraints and *RI* enhance realism but potentially reduce the quantity and severity of the identified test cases.

F. RQ4: Contribution of Interpretability Approach

1) *Methodology*: To answer RQ4, we begin by assessing the accuracy of the interpretable rules derived from the complete solutions by evaluating the *Mean Absolute Error (MAE)*. *MAE* is a widely used metric for evaluating the accuracy of predictive models, measuring the average magnitude of errors between predicted and actual values [91], [92]. In our context, *MAE* quantifies how accurately the interpretable rules characterize the differences in MR violations between two versions of the ADS under test. A lower *MAE* value indicates higher accuracy of the model in capturing the behavioral differences. Specifically, *MAE* calculates the mean of the absolute differences between each pair of predicted and true values:

$$MAE := \frac{1}{|\mathcal{SP}'|} \sum_{i \in \mathcal{SP}'} |y_i - \hat{y}_i|$$

where \mathcal{SP}' denotes the set of complete solutions, y_i is the observed difference in MR violations for a given complete solution, and \hat{y}_i is the predicted value.

These findings emphasize the importance of selecting the appropriate configuration based on the testing objective in terms of prioritizing the realism, severity, or diversity of the discovered solutions.

We compare *RuleFit* used in *CoCoMagic* against two baseline methods, i.e., *Random Forest (RF)* and *Gradient Boosted Decision Tree (GBDT)*, both commonly used for regression tasks. All methods are trained on the same dataset of complete solutions, paired with their corresponding differences in MR violations. The dataset comprises two types of complete solutions. The first type includes solutions where the two systems exhibit observable behavioral differences. Each of these solutions is assigned a fitness value that reflects both the direction and severity of the difference, with positive values indicating better performance by the original system, while negative values suggest the updated system fares better. The second type consists of solutions where no behavioral difference is observed between the systems. These solutions are assigned a fitness value of zero. This combination allows the prediction methods to learn not only what conditions lead to discrepancies, but also which solutions result in consistent behavior across both versions. By training on this combined dataset, *RuleFit* and baseline methods can identify the conditions that cause the systems to diverge, while also recognizing when their behaviors remain the same. The combined dataset consists of 2,236 complete solutions, with 1,321 solutions exhibiting behavioral differences and 915 solutions showing no differences, split into 80% for training and 20% for validation. To account for randomness in training, each method is evaluated over 500 independent runs with different random seeds to ensure robustness and generalizability of the results. To facilitate interpretability, *RuleFit* is constrained to extract at most 30 rules per run. Since our goal is explanation rather than maximal predictive accuracy, a smaller, high-importance rule set is easier to audit and apply in practice. This threshold was chosen based on both empirical observations and human interpretability considerations. In preliminary experiments, we varied the maximum number of rules while keeping the dataset of complete solutions fixed and evaluated the resulting prediction accuracy. The model achieved its highest accuracy when the limit was set to approximately 30 rules. From a cognitive perspective, prior work on model interpretability suggests that human analysts can effectively process only a limited number of rules before comprehension and decision quality degrade [93]. Therefore, limiting the output to 30 rules preserves most of the explanatory power while keeping the results concise and practical for human review. For a fair comparison, the hyperparameters of the baseline methods were tuned using randomized search [94], a hyperparameter optimization technique that samples parameter configurations from predefined ranges, aiming to approximate the best-performing settings for each method on the dataset.

In addition to evaluating prediction accuracy, we assess the *support* of the extracted interpretable rules, which refers to the degree to which the rules support or cover the identified complete solutions and is essential for their practical usefulness. A complete solution is considered supported if there exists at least one rule whose conditions are satisfied by the solution. To understand how thoroughly the rules support the identified complete solutions with behavioral differences (1,321 solutions), we analyze the distribution of the *support* of the rules across 500 independent runs of *RuleFit*. Specifically, in each run, we

compute the proportion of complete solutions that are supported by the full set of extracted rules. This analysis reveals the extent to which the rules capture the behavioral discrepancies reflected in the identified complete solutions. A higher proportion indicates stronger support or broader coverage, suggesting that the rules provide a more comprehensive explanation of the behavioral differences between the two system versions.

Finally, we present an example rule extracted from one of the *RuleFit* runs to demonstrate the interpretability and practical value of the generated rules. It showcases the effectiveness of the interpretability approach to gain a deeper understanding of the underlying factors contributing to the observed behavioral discrepancies.

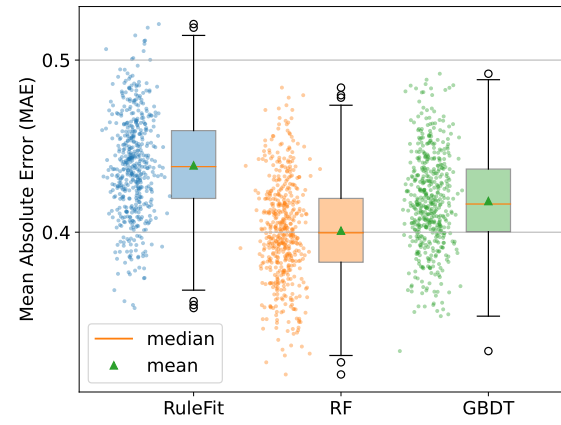


Fig. 9. Distribution of *Mean Absolute Error (MAE)* for *RuleFit* in *CoCoMagic* and baseline methods. A lower *MAE* value indicates higher accuracy of the model in capturing behavioral differences between the two system versions. Individual points beside each box represent the *MAE* values for each identified test case.

2) *Results*: Fig. 9 presents the distribution of *MAE* values for predictions made by *RuleFit* in *CoCoMagic* and the baseline methods, *RF* and *GBDT*. The results indicate that *RuleFit* achieves an average *MAE* value of 0.439, which is higher than that of *RF* (0.401) and *GBDT* (0.418). Although *RF* and *GBDT* yield slightly lower average *MAE* value, indicating higher accuracy in modeling behavioral differences in MR violations, they lack interpretability as they tend to generate a large number of complex rules. In decision tree-based models like *RF* and *GBDT*, these rules correspond to decision paths, which are sequences of feature-based conditions followed from the root to a leaf node in each tree. On average, *RF* produces 1009.99 such paths and *GBDT* produces 1589.00, making it difficult to extract clear, human-understandable insights from their predictions. This limitation reduces their practical usefulness for understanding the behavioral discrepancies between system versions. In contrast, *RuleFit* strikes a balance between accuracy and interpretability, producing a concise set of human-readable rules (28.64 rules on average) that facilitate understanding while still achieving accuracy close to that of *GBDT* and *RF*. Furthermore, the rules generated by *RF* and *GBDT* are more complex, averaging 3.78 and 3.27 conditions per rule, respectively, whereas *RuleFit* rules average only 2.12 conditions. This simplicity enhances the interpretability of *RuleFit* rules, making them more accessible for human analysts.

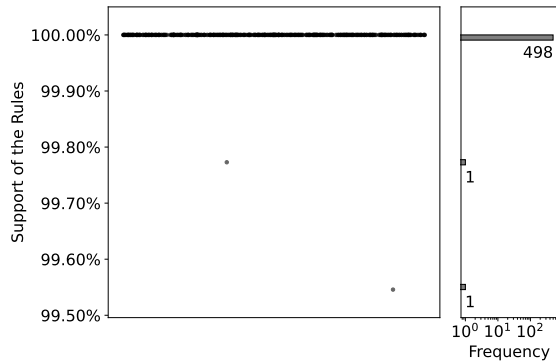


Fig. 10. Distribution of the *support* of the rules extracted by *RuleFit* in *CoCoMagic*. Higher *support* values indicate that the rules cover more complete solutions. The left subplot shows the distribution across all 500 runs, with horizontal jitter added to avoid overlapping points and improve visibility. The right subplot shows the same data as a histogram with a logarithmic scale for better visualization.

Fig. 10 shows the distribution of the *support* of the rules extracted by *RuleFit*, where each dot in the left subplot represents the *support* value of the full set of rules extracted in a single run. Horizontal jitter is applied to the dots in the left subplot to reduce overlap and improve clarity. The right subplot presents the same data as a histogram with a logarithmic scale on the x-axis to better visualize the distribution. The *support* distribution demonstrates that the rules extracted by *RuleFit* consistently cover nearly all of the identified complete solutions. In 498 out of 500 independent runs, the generated rules achieved 100% *support*, meaning every identified complete solution was covered by at least one rule. The remaining few runs show only minor deviations, with *support* values still exceeding 99.5%. Given the maximum of 30 rules allowed per run, the ability to achieve near-complete coverage of all identified solutions is particularly noteworthy. This high level of *support* underscores the effectiveness and consistency of *RuleFit* in capturing a compact yet comprehensive set of interpretable rules or patterns that explain the observed behavioral differences across diverse runs.

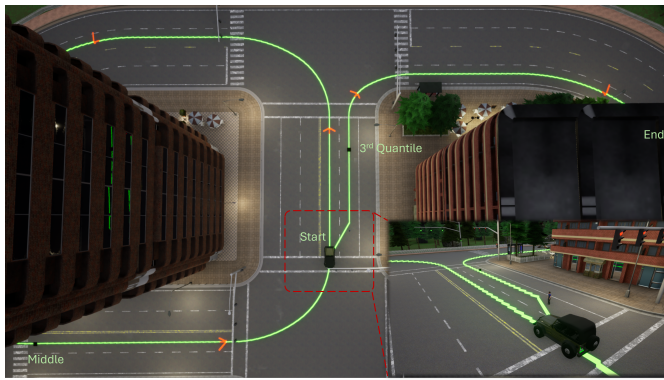


Fig. 11. An example scenario satisfying a representative rule extracted by *RuleFit* in *CoCoMagic*.

To further illustrate the practical value of this approach, we present a representative example from one of the runs. The representative rule is ranked as the most important among

all extracted rules. The rule states “IF the relative position of the ego vehicle during the third quartile of the trajectory is less than 23.78 meters to the left of its starting position in the source scenario, there are at most 16 static objects in the source scenario, and the relative position of the ego vehicle in the middle of the trajectory is less than 68.73 meters to the left of its starting position in the follow-up scenario, THEN the updated ADS tends to exhibit more MR violations than the original version, with a predicted difference of 0.492, supported by 71.03% of the identified complete solutions”. This rule captures a set of interacting spatial and contextual conditions under which the updated ADS is more likely to generate violations compared to the original. Each condition contributes an interpretable insight into when behavioral differences between the two versions are most likely to occur. An example scenario satisfying this rule is illustrated in Fig. 11. The first condition requires that, during the third quartile of the trajectory in the source scenario, the ego vehicle’s lateral displacement remains less than 23.78 meters to the left of its starting position. This suggests that the ego vehicle does not deviate substantially from its initial lane or execute a sharp left maneuver at this stage. The second condition constrains the source scenario itself, requiring that the number of static objects does not exceed 16, which limits the level of environmental complexity to a moderately challenging but not excessively congested scene. The third condition concerns the follow-up scenario, requiring that the ego vehicle’s lateral displacement at the midpoint of its trajectory is less than 68.73 meters to the left of its starting position. This indicates that the vehicle may have executed a left turn or a lane change in the middle of the trajectory, which could trigger different responses across the two system versions, possibly due to updated planning or lane-keeping mechanisms. Taken together, these spatial and contextual constraints highlight a systematic relationship between vehicle positioning and environmental structure, revealing conditions under which the updated ADS is more prone to generating MR violations than the original.

In summary, the results demonstrate that *RuleFit*, as used in *CoCoMagic*, effectively balances accuracy and interpretability in modeling behavioral differences in MR violations. It produces a compact set of human-readable rules with competitive accuracy, indicating a reliable ability to capture behavioral discrepancies. It also provides practical insights into whether and under which conditions the updated system exhibits more violations than the original, supporting informed decisions about real-world deployment. This approach provides interpretable and actionable explanations of the factors driving behavioral discrepancies, facilitating a more comprehensive understanding of system updates.

Answer to RQ4

In our interpretability approach, *RuleFit* effectively balances accuracy and interpretability when modeling differences in MR violations, producing a compact set of human-readable rules with accuracy comparable to *GBDT* and *RF*.

VI. DISCUSSION

A. Trade-offs in Using Constraints and the Population Initialization Strategy

In search-based generation of realistic and effective test cases, the use of constraints and the choice of population initialization strategy are critical factors shaping the realism, severity, and quantity of the resulting scenarios. These two factors influence the balance between producing test cases that closely reflect real-world conditions and exploring a wide range of potentially risky or severe behavioral discrepancies. Achieving this balance inevitably involves trade-offs. Tighter controls or heavy reliance on observed execution scenarios may improve realism but can limit the discovery of critical edge cases, whereas looser controls may enhance quantity but may reduce practical relevance.

Constraints guide the search toward regions of the solution space that are more relevant to real-world conditions. By penalizing unrealistic or infeasible conditions, they ensure that the generated test cases remain grounded in scenarios that could occur in practice. This targeted focus enhances the practical value of identified test cases by reducing time spent analyzing irrelevant or impossible cases. However, collecting a diverse and representative set of execution scenarios is important to capture the breadth of conditions under which failures may occur. Excessive similarity among collected execution scenarios can cause the testing process to miss distinct failure modes that may occur under different yet equally plausible conditions. Moreover, constraints that are too restrictive can narrow the search space excessively, omitting rare but potentially critical situations that might expose severe behavioral discrepancies. Conversely, relaxing the constraints expands exploration and increases the diversity of generated test cases, but at the cost of admitting unrealistic or invalid scenarios that require additional computational filtering. Based on our empirical findings, a constraint level that penalizes approximately 60–70% of candidate test cases per generation tends to strike an effective balance, maintaining both solution realism and sufficient severity.

Similarly, the population initialization strategy introduces its own set of trade-offs. Initializing the search with execution scenarios sampled from real-world data (i.e., the *RI* strategy) accelerates convergence by starting from scenarios already representative of operational contexts. This often yields test cases that are immediately applicable and realistic, making the approach well-suited when computational budgets or testing time are constrained. However, the drawback is that reliance on known scenarios can bias the search toward familiar behaviors, limiting the discovery of novel or unexpected situations that have not been previously observed but may reveal critical behavioral discrepancies. In contrast, a purely random initialization promotes broader exploration, improving the likelihood of uncovering rare, high-severity cases that challenge system safety or reliability. The trade-off is that such cases may be less realistic and, without a sufficiently diverse and complete set of representative execution scenarios, the search may overlook critical and realistic conditions that could lead to safety risks.

Selecting the right balance between constraints and initialization strategies depends on the specific objectives of the testing. Our experimental results (see Section V-E) show that combining constraints with *RI* produces test cases with the highest realism. However, this approach tends to limit the discovery of the most severe behavioral discrepancies. Therefore, practitioners must weigh the trade-offs carefully, tailoring their approach to ensure both targeted realism and adequate exploration to effectively identify potential behavioral discrepancies and safety issues.

B. Threats to Validity

This section discusses potential threats to the validity of our results, following the classification into four categories: Internal, External, Construct, and Conclusion validity [95].

1) *Internal validity*: Internal validity reflects how reliably a study establishes a cause-and-effect relationship between the experiment and its outcomes. One potential threat is the sensitivity of population-based methods (i.e., *CoCoMagic* and *SGA*) to hyperparameter settings. The chosen configurations may not be optimal, which could affect performance. To address this, we adopted widely recommended hyperparameter values from the literature [87]. For parameters lacking established defaults, we selected values based on a pilot experiment.

Another internal validity concern stems from slight mismatches between the actual number of executed simulations and the allocated simulation budgets for the population-based methods. We mitigated this issue by applying linear interpolation to align simulation budgets across different methods. However, interpolation assumes a linear and continuous relationship between metrics and the search budget. This assumption may not hold if metrics exhibit abrupt or non-linear changes across budgets, which could lead to inaccuracies in the aligned results. To reduce this risk, we validated the interpolation by analyzing metric trends and confirming that the linear assumption was reasonable within the tested budget range.

A further threat involves the correctness and reliability of the MRs used to detect behavioral differences. Since MRs serve as the basis for identifying violations, any inaccuracies, such as overly strict conditions, could result in false positives or negatives. To address this, we used well-established MRs from prior studies and conducted a pilot experiment to validate them. During this phase, we analyzed unexpected results and adjusted parameters to ensure the MRs were calibrated correctly. This refinement process helped ensure the reliability of the MRs in the main experiments.

2) *External validity*: External validity concerns the extent to which the results can be generalized to other contexts, particularly the applicability of results beyond the specific simulation environment used in this study. Due to the enormous effort and computation time involved in preparing and running our experiments, a primary threat to external validity arises from our reliance on a single ADS (INTERFUSER) and a specific simulator (CARLA) for the case study. For example, the substantial engineering effort required to enable seamless scenario execution using CARLA and INTERFUSER constrained our ability to include additional platforms. While this choice may limit generalizability, both technologies are widely recognized

within the autonomous driving research community. CARLA is an open-source, high-fidelity simulator extensively used in academia and industry, and INTERFUSER ranked among the top-performing systems on the CARLA *Leaderboard* during the evaluation period.

Another potential threat lies in the representativeness of the execution scenarios used. If the scenarios do not sufficiently reflect the variability of real-world driving conditions, the findings may lack general applicability. To mitigate this concern, we leveraged a variety of maps contributed by the CARLA community, encompassing diverse urban layouts, road geometries, and traffic conditions. We executed the ADS in these environments and systematically collected execution scenarios at five-second intervals to ensure coverage of different driving situations, including variations in traffic density, weather, and road types. From the collected execution scenarios, we randomly sampled a total of 800 scenarios, distributed equally across all maps, for use in our experiments. This sampling strategy aimed to ensure broad scenario diversity and better reflect the range of conditions encountered in real-world autonomous driving, thereby improving the generalizability of our results.

3) *Construct validity*: Construct validity concerns the extent to which the measurements used in a study accurately reflect the theoretical constructs they are intended to represent. In our work, a central concern is whether the *DS* metric appropriately captures the effectiveness of each method in identifying differences in MR violations and in exploring diverse regions of the search space. Although this metric is designed to reflect these aspects, it may not fully encompass all dimensions of solution quality or diversity.

4) *Conclusion validity*: Conclusion validity refers to the extent to which a research conclusion can be trusted. A notable limitation in our experiments is the relatively small number of repetitions, i.e., 10 runs per method, due to the substantial computational costs involved. To mitigate the risk of statistical error from this limited sample size, we report descriptive statistics along with their corresponding confidence intervals. This approach helps convey both the central trends and the uncertainty in the results, providing a more reliable basis for interpreting our findings.

VII. CONCLUSION

In this paper, we presented *CoCoMagic*, a novel automated testing method that integrates Differential Testing (DT), Metamorphic Testing (MT), and advanced search-based testing to assess the overall impact of updates on AS behavior. By leveraging MT, *CoCoMagic* effectively identifies test cases that expose behavioral discrepancies between system versions, which may lead to safety violations. Its cooperative co-evolutionary approach efficiently explores the high-dimensional search space, directing the search toward test cases most likely to reveal significant behavioral differences. The use of constraints and population generation strategies favors the generation of test cases that reflect realistic operating conditions and remain applicable to practical scenarios. The interpretability approach we propose complements this process by providing

clear insights into the underlying causes of identified discrepancies, enabling developers to better understand and mitigate potential safety risks.

Our evaluation on the CARLA simulator with the INTERFUSER ADS shows that *CoCoMagic* consistently outperforms baseline methods across diverse budget and threshold settings, efficiently generating severe test cases that uncover important behavioral differences between system versions. These findings indicate that *CoCoMagic* offers an effective and efficient solution for AS differential testing in open contexts by decomposing the high-dimensional search space through cooperative co-evolution. The realism of the generated scenarios, combined with the explanatory power of the interpretability approach, makes *CoCoMagic* a practical and actionable tool for developers aiming to improve the safety and reliability of evolving ASs.

DATA AVAILABILITY

The replication package for our experiments, which includes the implementation of our approach, baseline methods, configuration files, and experimental results, will be made available on Figshare upon acceptance of our paper.

ACKNOWLEDGMENTS

This work was supported by a research grant from Huawei Technologies Canada Co., Ltd, as well as the Canada Research Chair and Discovery Grant programs of the Natural Sciences and Engineering Research Council of Canada (NSERC). Lionel C. Briand's contribution was partially funded by the Research Ireland grant 13/RC/209.

REFERENCES

- [1] S. Tang, Z. Zhang, Y. Zhang, J. Zhou, Y. Guo, S. Liu, S. Guo, Y.-F. Li, L. Ma, Y. Xue, and Y. Liu, "A survey on automated driving system testing: Landscapes and trends," *ACM Transactions on Software Engineering and Methodology*, vol. 32, no. 5, pp. 1–62, Jul. 2023. [Online]. Available: <http://dx.doi.org/10.1145/3579642>
- [2] F. Khan, M. Falco, H. Anwar, and D. Pfahl, "Safety testing of automated driving systems: A literature review," *IEEE Access*, vol. 11, pp. 120 049–120 072, Oct. 2023. [Online]. Available: <http://dx.doi.org/10.1109/ACCESS.2023.3327918>
- [3] G. Lou, Y. Deng, X. Zheng, M. Zhang, and T. Zhang, "Testing of autonomous driving systems: where are we and where should we go?" in *Proceedings of the 30th ACM Joint European Software Engineering Conference and Symposium on the Foundations of Software Engineering*, ser. ESEC/FSE '22. New York, NY, USA: Association for Computing Machinery, Nov. 2022, pp. 31–43. [Online]. Available: <http://dx.doi.org/10.1145/3540250.3549111>
- [4] L. Yang, Y. Li, D. Huang, and J. Xia, "Iterative learning of an unknown road path through cooperative driving of vehicles," *IET Intelligent Transport Systems*, vol. 14, pp. 423–431, Mar. 2020. [Online]. Available: <http://dx.doi.org/10.1049/iet-its.2019.0411>
- [5] X. Li, C. Liu, B. Chen, and J. Jiang, "Robust adaptive learning-based path tracking control of autonomous vehicles under uncertain driving environments," *IEEE Transactions on Intelligent Transportation Systems*, vol. 23, no. 11, pp. 20 798–20 809, Nov. 2022. [Online]. Available: <http://dx.doi.org/10.1109/TITS.2022.3176970>
- [6] Y. Yao, "Enhancing autonomous driving systems with deep learning and spatial channel attention mechanisms: an experimental study," in *Fourth International Conference on Machine Learning and Computer Application*, ser. ICMLCA '23, X. Yao and X. Kong, Eds., vol. 13176, International Society for Optics and Photonics. SPIE, May 2024, p. 131761L. [Online]. Available: <https://doi.org/10.1117/12.3029174>

- [7] G. Fraser and A. Arcuri, "Whole test suite generation," *IEEE Transactions on Software Engineering*, vol. 39, no. 2, pp. 276–291, Feb. 2013. [Online]. Available: <http://dx.doi.org/10.1109/TSE.2012.14>
- [8] V. Riccio, G. Jahangirova, A. Stocco, N. Humbatova, M. Weiss, and P. Tonella, "Testing machine learning based systems: a systematic mapping," *Empirical Software Engineering*, vol. 25, no. 6, pp. 5193–5254, Sep. 2020. [Online]. Available: <https://doi.org/10.1007/s10664-020-09881-0>
- [9] T. Y. Chen, F.-C. Kuo, H. Liu, P.-L. Poon, D. Towey, T. H. Tse, and Z. Q. Zhou, "Metamorphic testing: A review of challenges and opportunities," *ACM Computing Surveys*, vol. 51, no. 1, pp. 1–27, Jan. 2018. [Online]. Available: <https://doi.org/10.1145/3143561>
- [10] Z. Q. Zhou and L. Sun, "Metamorphic testing of driverless cars," *Communications of the ACM*, vol. 62, no. 3, pp. 61–67, 2019.
- [11] S. Burton, I. Habli, T. Lawton, J. McDermid, P. Morgan, and Z. Porter, "Mind the gaps: Assuring the safety of autonomous systems from an engineering, ethical, and legal perspective," *Artificial Intelligence*, vol. 279, p. 103201, Feb. 2020. [Online]. Available: <http://dx.doi.org/10.1016/j.artint.2019.103201>
- [12] A. Dosovitskiy, G. Ros, F. Codevilla, A. Lopez, and V. Koltun, "CARLA: An open urban driving simulator," in *Proceedings of the 1st Annual Conference on Robot Learning*, ser. Proceedings of Machine Learning Research, vol. 78. PMLR, Nov. 2017, pp. 1–16. [Online]. Available: <https://proceedings.mlr.press/v78/dosovitskiy17a.html>
- [13] H. Shao, L. Wang, R. Chen, H. Li, and Y. Liu, "Safety-enhanced autonomous driving using interpretable sensor fusion transformer," in *Proceedings of The 6th Conference on Robot Learning*, ser. Proceedings of Machine Learning Research, K. Liu, D. Kulic, and J. Ichniowski, Eds., vol. 205. PMLR, Dec. 2023, pp. 726–737. [Online]. Available: <https://proceedings.mlr.press/v205/shao23a.html>
- [14] H. Yousefizadeh, S. Gu, L. C. Briand, and A. Nasr, "Using cooperative co-evolutionary search to generate metamorphic test cases for autonomous driving systems," *IEEE Transactions on Software Engineering*, pp. 1–30, 2025. [Online]. Available: <http://dx.doi.org/10.1109/TSE.2025.3570897>
- [15] R. B. Abdessalem, S. Nejati, L. C. Briand, and T. Stifter, "Testing advanced driver assistance systems using multi-objective search and neural networks," in *Proceedings of the 31st IEEE/ACM International Conference on Automated Software Engineering*, ser. ASE '16. New York, NY, USA: Association for Computing Machinery, Aug. 2016, pp. 63–74. [Online]. Available: <http://dx.doi.org/10.1145/2970276.2970311>
- [16] R. B. Abdessalem, S. Nejati, L. C. Briand, and T. Stifter, "Testing autonomous cars for feature interaction failures using many-objective search," in *Proceedings of the 33rd ACM/IEEE International Conference on Automated Software Engineering*, ser. ASE '18. New York, NY, USA: Association for Computing Machinery, Sep. 2018, pp. 143–154. [Online]. Available: <http://dx.doi.org/10.1145/3238147.3238192>
- [17] R. B. Abdessalem, S. Nejati, L. C. Briand, and T. Stifter, "Testing vision-based control systems using learnable evolutionary algorithms," in *Proceedings of the 40th International Conference on Software Engineering*, ser. ICSE '18. New York, NY, USA: Association for Computing Machinery, May 2018, pp. 1016–1026. [Online]. Available: <http://dx.doi.org/10.1145/3180155.3180160>
- [18] T. Dreossi, A. Donzé, and S. A. Seshia, "Compositional falsification of cyber-physical systems with machine learning components," *Journal of Automated Reasoning*, vol. 63, no. 4, pp. 1031–1053, Jan. 2019. [Online]. Available: <http://dx.doi.org/10.1007/s10817-018-09509-5>
- [19] L. V. Sartori, "Simulation-based testing to improve safety of autonomous robots," in *2019 IEEE International Symposium on Software Reliability Engineering Workshops*, ser. ISSREW '19. Institute of Electrical and Electronics Engineers (IEEE), Oct. 2019, pp. 104–107. [Online]. Available: <http://dx.doi.org/10.1109/ISSREW.2019.00053>
- [20] F. U. Haq, D. Shin, and L. Briand, "Efficient online testing for dnn-enabled systems using surrogate-assisted and many-objective optimization," in *Proceedings of the 44th International Conference on Software Engineering*, ser. ICSE '22. New York, NY, USA: Association for Computing Machinery, May 2022, pp. 811–822. [Online]. Available: <http://dx.doi.org/10.1145/3510003.3510188>
- [21] N. Kolb, F. Hauer, and A. Pretschner, "Fitness function templates for testing automated and autonomous driving systems in intersection scenarios," in *2021 IEEE International Intelligent Transportation Systems Conference*, ser. ITSC '21. Institute of Electrical and Electronics Engineers (IEEE), Sep. 2021, pp. 217–222. [Online]. Available: <http://dx.doi.org/10.1109/ITSC48978.2021.9564591>
- [22] F. Hauer, A. Pretschner, and B. Holzmüller, "Fitness functions for testing automated and autonomous driving systems," in *Computer Safety, Reliability, and Security*, ser. SAFECOMP '19. Springer International Publishing, Aug. 2019, pp. 69–84. [Online]. Available: http://dx.doi.org/10.1007/978-3-030-26601-1_5
- [23] Y. Luo, X.-Y. Zhang, P. Arcaini, Z. Jin, H. Zhao, F. Ishikawa, R. Wu, and T. Xie, "Targeting requirements violations of autonomous driving systems by dynamic evolutionary search," in *2021 36th IEEE/ACM International Conference on Automated Software Engineering*, ser. ASE '21. Institute of Electrical and Electronics Engineers (IEEE), Nov. 2021, pp. 279–291. [Online]. Available: <http://dx.doi.org/10.1109/ASE51524.2021.9678883>
- [24] C. Birchler, N. Ganz, S. Khatiri, A. Gambi, and S. Panichella, "Cost-effective simulation-based test selection in self-driving cars software," *Science of Computer Programming*, vol. 226, p. 102926, Mar. 2023. [Online]. Available: <http://dx.doi.org/10.1016/j.scico.2023.102926>
- [25] C. Birchler, S. Khatiri, P. Derakhshanfar, S. Panichella, and A. Panichella, "Single and multi-objective test cases prioritization for self-driving cars in virtual environments," *ACM Transactions on Software Engineering and Methodology*, vol. 32, no. 2, pp. 1–30, Apr. 2023. [Online]. Available: <http://dx.doi.org/10.1145/3533818>
- [26] S. Khatiri, S. Panichella, and P. Tonella, "Simulation-based test case generation for unmanned aerial vehicles in the neighborhood of real flights," in *2023 IEEE Conference on Software Testing, Verification and Validation*, ser. ICST '23. Institute of Electrical and Electronics Engineers (IEEE), Apr. 2023, pp. 281–292. [Online]. Available: <http://dx.doi.org/10.1109/ICST57152.2023.00034>
- [27] G. K. G. Shimanuki, A. M. Nascimento, L. F. Vismari, J. B. C. Junior, J. R. de Almeida Junior, and P. S. Cugnasca, "CORTEX-AVD: A framework for CORner case testing and EXploration in autonomous vehicle development," 2025. [Online]. Available: <https://arxiv.org/abs/2504.03989>
- [28] D. J. Fremont, T. Dreossi, S. Ghosh, X. Yue, A. L. Sangiovanni-Vincentelli, and S. A. Seshia, "Scenic: a language for scenario specification and scene generation," in *Proceedings of the 40th ACM SIGPLAN Conference on Programming Language Design and Implementation*, ser. PLDI '19. New York, NY, USA: Association for Computing Machinery (ACM), Jun. 2019, pp. 63–78. [Online]. Available: <https://doi.org/10.1145/3314221.3314633>
- [29] G. Li, Y. Li, S. Jha, T. Tsai, M. Sullivan, S. K. S. Hari, Z. Kalbarczyk, and R. Iyer, "AV-FUZZER: Finding safety violations in autonomous driving systems," in *2020 IEEE 31st International Symposium on Software Reliability Engineering*, ser. ISSRE '20. Institute of Electrical and Electronics Engineers (IEEE), Oct. 2020, pp. 25–36. [Online]. Available: <http://dx.doi.org/10.1109/ISSRE5003.2020.00012>
- [30] Baidu. Apollo. [Online]. Available: <https://en.apollo.auto/apollo-self-driving>
- [31] M. Cheng, Y. Zhou, and X. Xie, "BehAVExplor: Behavior diversity guided testing for autonomous driving systems," in *Proceedings of the 32nd ACM SIGSOFT International Symposium on Software Testing and Analysis*, ser. ISSTA '23. New York, NY, USA: Association for Computing Machinery (ACM), Jul. 2023, pp. 488–500. [Online]. Available: <https://doi.org/10.1145/3597926.3598072>
- [32] G. Rong, B. H. Shin, H. Tabatabaei, Q. Lu, S. Lemke, M. Mozeiko, E. Boise, G. Uhm, M. Gerow, S. Mehta, E. Agafonov, T. H. Kim, E. Stern, K. Ushiroda, M. Reyes, D. Zelenkovsky, and S. Kim, "LGSVL simulator: A high fidelity simulator for autonomous driving," in *2020 IEEE 23rd International Conference on Intelligent Transportation Systems*, ser. ITSC '20. Institute of Electrical and Electronics Engineers (IEEE), Sep. 2020, pp. 1–6. [Online]. Available: <http://dx.doi.org/10.1109/ITSC45102.2020.9294422>
- [33] V. Crespo-Rodriguez, Neelofar, and A. Aleti, "PAFOT: A position-based approach for finding optimal tests of autonomous vehicles," in *Proceedings of the 5th ACM/IEEE International Conference on Automation of Software Test*, ser. AST '24. New York, NY, USA: Association for Computing Machinery (ACM), Apr. 2024, pp. 159–170. [Online]. Available: <http://dx.doi.org/10.1145/3644032.3644457>
- [34] X. Ji, L. Xue, Z. He, and X. Luo, "Autonomous driving system testing via diversity-oriented driving scenario exploration," *ACM Transactions on Software Engineering and Methodology*, Apr. 2025. [Online]. Available: <https://doi.org/10.1145/3727875>
- [35] CARLA. CARLA autonomous driving leaderboard. [Online]. Available: <https://leaderboard.carla.org/leaderboard/>
- [36] A. Gambi, M. Mueller, and G. Fraser, "Automatically testing self-driving cars with search-based procedural content generation," in *Proceedings of the 28th ACM SIGSOFT International Symposium on Software Testing and Analysis*, ser. ISSTA '19, vol. 4. New York, NY, USA: Association for Computing Machinery, Jul. 2019, pp. 318–328. [Online]. Available: <http://dx.doi.org/10.1145/3293882.3330566>
- [37] Q. Goss and M. I. Akbas, "Eagle strategy with local search for scenario based validation of autonomous vehicles," in *2022 International*

- Conference on Connected Vehicle and Expo*, ser. ICCVE '22. Institute of Electrical and Electronics Engineers (IEEE), Mar. 2022, pp. 1–6. [Online]. Available: <http://dx.doi.org/10.1109/ICCVE52871.2022.9743067>
- [38] X. Zheng, H. Liang, B. Yu, B. Li, S. Wang, and Z. Chen, “Rapid generation of challenging simulation scenarios for autonomous vehicles based on adversarial test,” in *2020 IEEE International Conference on Mechatronics and Automation*, ser. ICMA '20. Institute of Electrical and Electronics Engineers (IEEE), Oct. 2020, pp. 1166–1172. [Online]. Available: <http://dx.doi.org/10.1109/ICMA49215.2020.9233535>
- [39] D. Humeniuk, F. Khomh, and G. Antoniol, “AmbieGen: A search-based framework for autonomous systems testing,” *Science of Computer Programming*, vol. 230, p. 102990, Aug. 2023. [Online]. Available: <http://dx.doi.org/10.1016/j.scico.2023.102990>
- [40] —, “Reinforcement learning informed evolutionary search for autonomous systems testing,” *ACM Transactions on Software Engineering and Methodology*, vol. 33, no. 8, Nov. 2024. [Online]. Available: <http://dx.doi.org/10.1145/3680468>
- [41] M. Biagiola, A. Stocco, V. Riccio, and P. Tonella, “Two is better than one: digital siblings to improve autonomous driving testing,” *Empirical Software Engineering*, vol. 29, no. 4, May 2024. [Online]. Available: <https://doi.org/10.1007/s10664-024-10458-4>
- [42] L. Sorokin, M. Biagiola, and A. Stocco, “Simulator ensembles for trustworthy autonomous driving testing,” 2025. [Online]. Available: <https://arxiv.org/abs/2503.08936>
- [43] Q. Pan, T. Wang, J. Ma, P. Arcaini, and T. Yue, “Simulation-based safety assessment of vehicle characteristics variations in autonomous driving systems,” *ACM Transactions on Software Engineering and Methodology*, Jun. 2025. [Online]. Available: <https://doi.org/10.1145/3743673>
- [44] K. Deb, A. Pratap, S. Agarwal, and T. Meyarivan, “A fast and elitist multiobjective genetic algorithm: NSGA-II,” *IEEE Transactions on Evolutionary Computation*, vol. 6, no. 2, pp. 182–197, Apr. 2002. [Online]. Available: <http://dx.doi.org/10.1109/4235.996017>
- [45] T. Y. Chen, S. Cheung, and S. Yiu, “Metamorphic testing: A new approach for generating next test cases,” *CoRR*, vol. abs/2002.12543, Feb. 2020. [Online]. Available: <https://arxiv.org/abs/2002.12543>
- [46] S. Segura, D. Towsley, Z. Q. Zhou, and T. Y. Chen, “Metamorphic testing: Testing the untestable,” *IEEE Software*, vol. 37, no. 3, pp. 46–53, May 2020. [Online]. Available: <http://dx.doi.org/10.1109/MS.2018.2875968>
- [47] Z. Yang, S. Huang, C. Zheng, X. Wang, Y. Wang, and C. Xia, “MetaLiDAR: Automated metamorphic testing of lidar-based autonomous driving systems,” *Journal of Software: Evolution and Process*, vol. 36, no. 7, p. e2644, Dec. 2023. [Online]. Available: <http://dx.doi.org/10.1002/smr.2644>
- [48] Z. Yang, S. Huang, T. Bai, Y. Yao, Y. Wang, C. Zheng, and C. Xia, “MetaSem: metamorphic testing based on semantic information of autonomous driving scenes,” *Software Testing, Verification and Reliability*, vol. 34, no. 5, p. e1878, May 2024. [Online]. Available: <http://dx.doi.org/10.1002/stvr.1878>
- [49] M. Lindvall, A. Porter, G. Magnusson, and C. Schulze, “Metamorphic model-based testing of autonomous systems,” in *2017 IEEE/ACM 2nd International Workshop on Metamorphic Testing*, ser. MET '17. Institute of Electrical and Electronics Engineers (IEEE), May 2017, pp. 35–41. [Online]. Available: <http://dx.doi.org/10.1109/MET.2017.6>
- [50] Y. Tian, K. Pei, S. Jana, and B. Ray, “DeepTest: automated testing of deep-neural-network-driven autonomous cars,” in *Proceedings of the 40th International Conference on Software Engineering*, ser. ICSE '18. New York, NY, USA: Association for Computing Machinery, May 2018, pp. 303–314. [Online]. Available: <http://dx.doi.org/10.1145/3180155.3180220>
- [51] M. Zhang, Y. Zhang, L. Zhang, C. Liu, and S. Khurshid, “DeepRoad: Gan-based metamorphic testing and input validation framework for autonomous driving systems,” in *Proceedings of the 33rd ACM/IEEE International Conference on Automated Software Engineering*, ser. ASE '18. New York, NY, USA: Association for Computing Machinery, Sep. 2018, pp. 132–142. [Online]. Available: <http://dx.doi.org/10.1145/3238147.3238187>
- [52] Y. Pan, H. Ao, and Y. Fan, “Metamorphic testing for autonomous driving systems in fog based on quantitative measurement,” in *2021 IEEE 21st International Conference on Software Quality, Reliability and Security Companion*, ser. QRS-C '21. Institute of Electrical and Electronics Engineers (IEEE), Dec. 2021, pp. 30–37. [Online]. Available: <http://dx.doi.org/10.1109/QRS-C55045.2021.00015>
- [53] J. C. Han and Z. Q. Zhou, “Metamorphic fuzz testing of autonomous vehicles,” in *Proceedings of the IEEE/ACM 42nd International Conference on Software Engineering Workshops*, ser. ICSEW '20. New York, NY, USA: Association for Computing Machinery, Jun. 2020, pp. 380–385. [Online]. Available: <http://dx.doi.org/10.1145/3387940.3392252>
- [54] M. Cheng, Y. Zhou, X. Xie, J. Wang, G. Meng, and K. Yang, “Evaluating decision optimality of autonomous driving via metamorphic testing,” 2024. [Online]. Available: <https://arxiv.org/abs/2402.18393>
- [55] E. M. Fredericks, M. Jacobs, and B. DeVries, “Towards a metamorphic testing architecture for software-defined drone systems,” in *2024 11th International Conference on Software Defined Systems*, ser. SDS '24. Institute of Electrical and Electronics Engineers (IEEE), Dec. 2024, pp. 170–177. [Online]. Available: <http://dx.doi.org/10.1109/SDS64317.2024.10883896>
- [56] R. Li, H. Liu, P.-L. Poon, D. Towey, C.-A. Sun, Z. Zheng, Z. Q. Zhou, and T. Y. Chen, “Metamorphic relation generation: State of the art and research directions,” *ACM Transactions on Software Engineering and Methodology*, vol. 34, no. 5, May 2025. [Online]. Available: <https://doi.org/10.1145/3708521>
- [57] X. Ma, X. Li, Q. Zhang, K. Tang, Z. Liang, W. Xie, and Z. Zhu, “A survey on cooperative co-evolutionary algorithms,” *IEEE Transactions on Evolutionary Computation*, vol. 23, no. 3, pp. 421–441, Jun. 2019. [Online]. Available: <http://dx.doi.org/10.1109/TEVC.2018.2868770>
- [58] Z. Yang, K. Tang, and X. Yao, “Large scale evolutionary optimization using cooperative coevolution,” *Information Sciences*, vol. 178, no. 15, pp. 2985–2999, Aug. 2008. [Online]. Available: <http://dx.doi.org/10.1016/j.ins.2008.02.017>
- [59] L. Panait, S. Luke, and J. F. Harrison, “Archive-based cooperative coevolutionary algorithms,” in *Proceedings of the 8th annual conference on Genetic and evolutionary computation*, ser. GECCO '06. New York, NY, USA: Association for Computing Machinery, Jul. 2006, pp. 345–352. [Online]. Available: <http://dx.doi.org/10.1145/1143997.1144060>
- [60] Y. Deng, X. Zheng, T. Zhang, H. Liu, G. Lou, M. Kim, and T. Y. Chen, “A declarative metamorphic testing framework for autonomous driving,” *IEEE Transactions on Software Engineering*, vol. 49, no. 4, pp. 1964–1982, Apr. 2023. [Online]. Available: <http://dx.doi.org/10.1109/TSE.2022.3206427>
- [61] F. U. Haq, D. Shin, S. Nejati, and L. Briand, “Can offline testing of deep neural networks replace their online testing?: A case study of automated driving systems,” *Empirical Software Engineering*, vol. 26, no. 90, Jul. 2021. [Online]. Available: <http://dx.doi.org/10.1007/s10664-021-09982-4>
- [62] S. Sharifi, D. Shin, L. C. Briand, and N. Aschbacher, “Identifying the hazard boundary of ml-enabled autonomous systems using cooperative coevolutionary search,” *IEEE Transactions on Software Engineering*, vol. 49, no. 12, pp. 5120–5138, Dec. 2023. [Online]. Available: <http://dx.doi.org/10.1109/TSE.2023.3327575>
- [63] L. Bull, “Evolutionary computation in multi-agent environments: Partners,” in *Proceedings of the 7th International Conference on Genetic Algorithms*. Morgan Kaufmann, Jul. 1997, pp. 370–377.
- [64] —, *Evolutionary computing in multi-agent environments: Operators*. Berlin, Heidelberg: Springer Berlin Heidelberg, 1998, pp. 43–52. [Online]. Available: <http://dx.doi.org/10.1007/BFb0040758>
- [65] R. P. Wiegand, W. C. Liles, and K. A. D. Jong, “An empirical analysis of collaboration methods in cooperative coevolutionary algorithms,” in *Proceedings of the genetic and evolutionary computation conference*, ser. GECCO '01, vol. 2611. Morgan Kaufmann, Jul. 2001, pp. 1235–1245.
- [66] D. R. Wilson and T. R. Martinez, “Improved heterogeneous distance functions,” *Journal of Artificial Intelligence Research*, vol. 6, pp. 1–34, Jan. 1997. [Online]. Available: <http://dx.doi.org/10.1613/jair.346>
- [67] A. Petrowski, “A clearing procedure as a niching method for genetic algorithms,” in *Proceedings of IEEE International Conference on Evolutionary Computation*, ser. ICEC '96. Institute of Electrical and Electronics Engineers (IEEE), May 1996, pp. 798–803. [Online]. Available: <http://dx.doi.org/10.1109/ICEC.1996.542703>
- [68] B. Sareni and L. Krahenbuhl, “Fitness sharing and niching methods revisited,” *IEEE Transactions on Evolutionary Computation*, vol. 2, no. 3, pp. 97–106, Sep. 1998. [Online]. Available: <http://dx.doi.org/10.1109/4235.735432>
- [69] M. Eigen, “Selforganization of matter and the evolution of biological macromolecules,” *Die Naturwissenschaften*, vol. 58, no. 10, pp. 465–523, Oct. 1971. [Online]. Available: <http://dx.doi.org/10.1007/BF00623322>
- [70] D. E. Goldberg and J. Richardson, “Genetic algorithms with sharing for multimodal function optimization,” in *Genetic algorithms and their applications: Proceedings of the Second International Conference on Genetic Algorithms*, vol. 4149. Hillsdale, NJ: Lawrence Erlbaum, 1987.
- [71] J. Horn and D. E. Goldberg, *A timing analysis of convergence to fitness sharing equilibrium*. Berlin, Heidelberg: Springer Science and Business Media LLC, 1998, pp. 23–33. [Online]. Available: <http://dx.doi.org/10.1007/BFb0056846>
- [72] S. W. Mahfoud, “Population size and genetic drift in fitness sharing,” in *Foundations of Genetic Algorithms*. Elsevier BV, 1995, vol. 3, pp. 185–

- [223] [Online]. Available: <http://dx.doi.org/10.1016/B978-1-55860-356-1.50014-5>
- [73] S. Luke, *Essentials of Metaheuristics*, 2nd ed. Lulu, 2013, available for free at <http://cs.gmu.edu/~sean/book/metaheuristics/>.
- [74] C. Mandrioli, S. Y. Shin, D. Bianculli, and L. Briand, “Testing CPS with design assumptions-based metamorphic relations and genetic programming,” *IEEE Transactions on Software Engineering*, pp. 1–19, Apr. 2025. [Online]. Available: <http://dx.doi.org/10.1109/TSE.2025.3563121>
- [75] J. H. Friedman and B. E. Popescu, “Predictive learning via rule ensembles,” *The Annals of Applied Statistics*, vol. 2, no. 3, pp. 916–954, Sep. 2008. [Online]. Available: <http://dx.doi.org/10.1214/07-AOAS148>
- [76] V. Margot and G. Luta, “A new method to compare the interpretability of rule-based algorithms,” *AI*, vol. 2, no. 4, pp. 621–635, Nov. 2021. [Online]. Available: <http://dx.doi.org/10.3390/ai2040037>
- [77] R. Tibshirani, “Regression shrinkage and selection via the lasso,” *Journal of the Royal Statistical Society Series B: Statistical Methodology*, vol. 58, no. 1, pp. 267–288, Jan. 1996. [Online]. Available: <http://dx.doi.org/10.1111/j.2517-6161.1996.tb02080.x>
- [78] J. H. Holland, *Adaptation in natural and artificial systems: an introductory analysis with applications to biology, control, and artificial intelligence*. MIT press, 1992.
- [79] A. Dosovitskiy, G. Ros, F. Codevilla, A. Lopez, and V. Koltun, “CARLA: An open urban driving simulator,” in *Proceedings of the 1st Annual Conference on Robot Learning*, ser. Proceedings of Machine Learning Research, S. Levine, V. Vanhoucke, and K. Goldberg, Eds., vol. 78. PMLR, Nov. 2017, pp. 1–16. [Online]. Available: <https://proceedings.mlr.press/v78/dosovitskiy17a.html>
- [80] Y. Deng, G. Lou, X. Zheng, T. Zhang, M. Kim, H. Liu, C. Wang, and T. Y. Chen, “BMT: Behavior driven development-based metamorphic testing for autonomous driving models,” in *2021 IEEE/ACM 6th International Workshop on Metamorphic Testing*, ser. MET ’21. Institute of Electrical and Electronics Engineers (IEEE), Jun. 2021, pp. 32–36. [Online]. Available: <http://dx.doi.org/10.1109/MET52542.2021.00012>
- [81] M. Iqbal, “Metamorphic relations for testing automated and autonomous driving systems and simulation platforms,” Ph.D. dissertation, School of Computing and Information Technology, University of Wollongong, 2024, doctor of Philosophy thesis. [Online]. Available: <https://ro.uow.edu.au/theses1/1758>
- [82] R. B. Abdessalem, A. Panichella, S. Nejati, L. C. Briand, and T. Stifter, “Automated repair of feature interaction failures in automated driving systems,” in *Proceedings of the 29th ACM SIGSOFT International Symposium on Software Testing and Analysis*, ser. ISSTA ’20. New York, NY, USA: Association for Computing Machinery, Jul. 2020, pp. 88–100. [Online]. Available: <http://dx.doi.org/10.1145/3395363.3397386>
- [83] T. Chugh, K. Sindhya, J. Hakanen, and K. Miettinen, “A survey on handling computationally expensive multiobjective optimization problems with evolutionary algorithms,” *Soft Computing*, vol. 23, no. 9, pp. 3137–3166, Dec. 2017. [Online]. Available: <http://dx.doi.org/10.1007/s00500-017-2965-0>
- [84] D. Whitley, *Next Generation Genetic Algorithms: A User’s Guide and Tutorial*. Springer International Publishing, Sep. 2018, pp. 245–274. [Online]. Available: http://dx.doi.org/10.1007/978-3-319-91086-4_8
- [85] Y. Lavinas, C. Aranha, T. Sakurai, and M. Ladeira, “Experimental analysis of the tournament size on genetic algorithms,” in *2018 IEEE International Conference on Systems, Man, and Cybernetics*, ser. SMC ’18. Institute of Electrical and Electronics Engineers (IEEE), Oct. 2018, pp. 3647–3653. [Online]. Available: <http://dx.doi.org/10.1109/SMC.2018.00617>
- [86] P. Kaelo and M. Ali, “Integrated crossover rules in real coded genetic algorithms,” *European Journal of Operational Research*, vol. 176, no. 1, pp. 60–76, Jan. 2007. [Online]. Available: <http://dx.doi.org/10.1016/j.ejor.2005.07.025>
- [87] S. Mirjalili, *Genetic Algorithm*. Springer International Publishing, Jun. 2018, pp. 43–55. [Online]. Available: http://dx.doi.org/10.1007/978-3-319-93025-1_4
- [88] S. Sette and L. Boullart, “Genetic programming: principles and applications,” *Engineering Applications of Artificial Intelligence*, vol. 14, no. 6, pp. 727–736, Dec. 2001. [Online]. Available: [http://dx.doi.org/10.1016/S0952-1976\(02\)00013-1](http://dx.doi.org/10.1016/S0952-1976(02)00013-1)
- [89] H. B. Mann and D. R. Whitney, “On a test of whether one of two random variables is stochastically larger than the other,” *The Annals of Mathematical Statistics*, vol. 18, no. 1, pp. 50–60, Mar. 1947. [Online]. Available: <http://dx.doi.org/10.1214/aoms/117730491>
- [90] F. Wilcoxon, “Individual comparisons by ranking methods,” *Biometrics Bulletin*, vol. 1, no. 6, pp. 80–83, Dec. 1945. [Online]. Available: <http://dx.doi.org/10.2307/3001968>
- [91] C. J. Willmott and K. Matsuura, “Advantages of the mean absolute error (MAE) over the root mean square error (RMSE) in assessing average model performance,” *Climate Research*, vol. 30, pp. 79–82, 2005. [Online]. Available: <http://dx.doi.org/10.3354/cr030079>
- [92] R. J. Hyndman and A. B. Koehler, “Another look at measures of forecast accuracy,” *International Journal of Forecasting*, vol. 22, no. 4, pp. 679–688, Oct. 2006. [Online]. Available: <http://dx.doi.org/10.1016/j.ijforecast.2006.03.001>
- [93] H. Lakkaraju, S. H. Bach, and J. Leskovec, “Interpretable decision sets: A joint framework for description and prediction,” in *Proceedings of the 22nd ACM SIGKDD International Conference on Knowledge Discovery and Data Mining*, ser. KDD ’16. New York, NY, USA: Association for Computing Machinery (ACM), Aug. 2016, pp. 1675–1684. [Online]. Available: <http://dx.doi.org/10.1145/2939672.2939874>
- [94] J. Bergstra and Y. Bengio, “Random search for hyper-parameter optimization,” *Journal of Machine Learning Research*, vol. 13, no. null, pp. 281–305, Feb. 2012.
- [95] C. Wohlin, P. Runeson, M. Höst, M. C. Ohlsson, B. Regnell, and A. Wesslén, *Experimentation in Software Engineering*. Berlin, Heidelberg: Springer Science and Business Media LLC, Sep. 2024. [Online]. Available: <http://dx.doi.org/10.1007/978-3-662-69306-3>

APPENDIX

EXPERIMENTAL RESULTS ON GP_2

Based on GP_2 , Fig. 12 compares the number of distinct solutions (DS) obtained by *CoCoMagic*, *SGA*, and *RS* over 10 runs. The x-axis shows the distance threshold θ_d , while the y-axis reports the average DS , with 95% confidence intervals as error bars. Results are shown across multiple fitness thresholds θ_f .

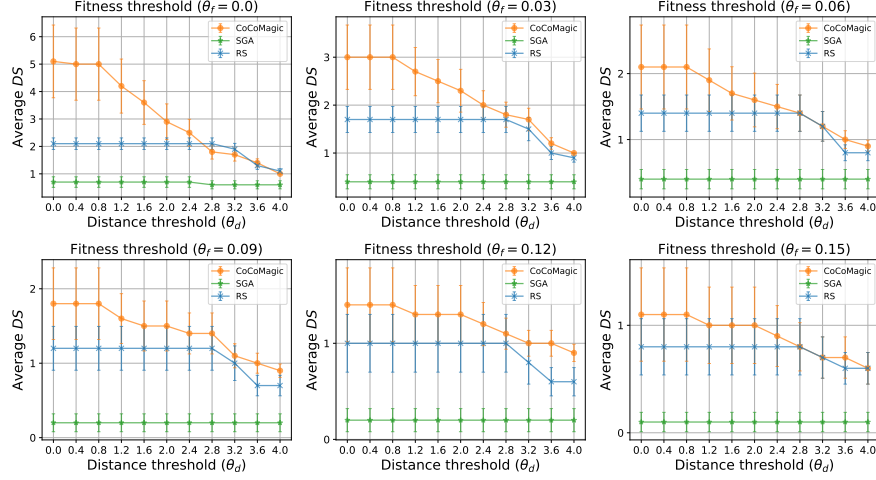


Fig. 12. *Distinct Solutions (DS)* vs. distance threshold (θ_d) across different fitness thresholds (θ_f). A higher DS value indicates that more distinct test cases have been discovered by the method. Each curve plots the average DS value at different θ_d settings, under a specific fitness threshold θ_f . This figure reveals how each method balances the quantity and diversity of test cases as θ_f varies.

Fig. 13 illustrates the progression of DS as the simulation budget increases for GP_2 . Each subplot corresponds to a specific combination of θ_f and θ_d , with distinct curves for *CoCoMagic*, *SGA*, and *RS*. Similar to GP1, the plots suggest differences in efficiency as methods uncover severe and diverse behavioral discrepancies over time.

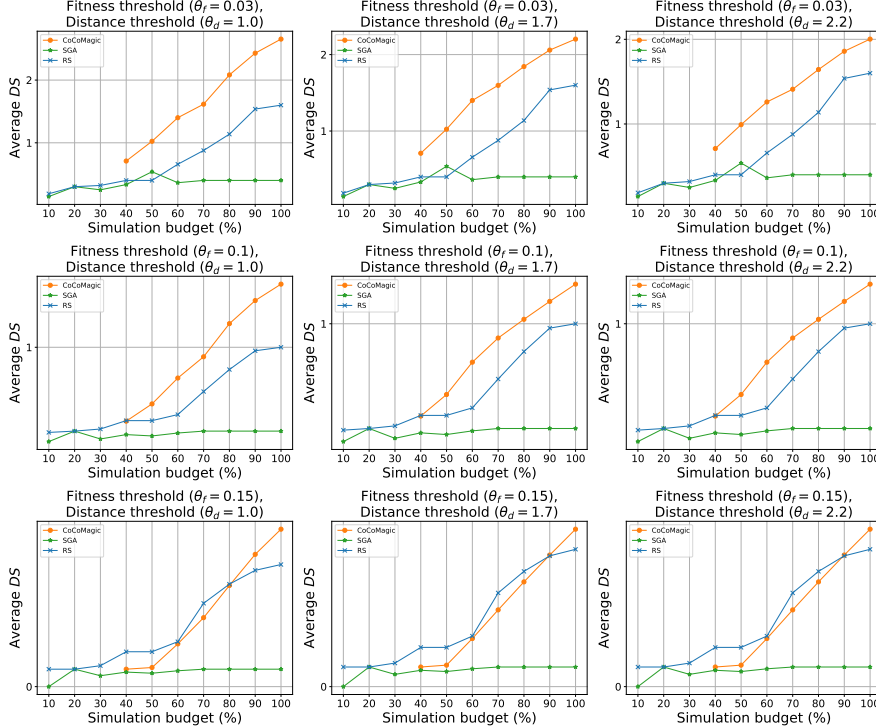


Fig. 13. *Distinct Solutions (DS)* progression across simulation budget levels. Each subplot illustrates how the DS value grows as more simulation resources are consumed, under specific combinations of fitness thresholds (θ_f) and distance thresholds (θ_d). The curves represent different methods, allowing a direct comparison of how quickly and effectively each approach uncovers severe and diverse behavioral discrepancies between ADS versions. Sharper increases and higher endpoints indicate greater efficiency in identifying test cases early in the search process.

Finally, Fig. 14 presents the distribution of execution times (in hours) for *CoCoMagic*, *SGA*, and *RS* under a fixed search budget in GP_2 . Similar to GP_1 , each boxplot summarizes results across 10 runs, enabling a comparison of computational efficiency, where shorter times indicate faster completion.

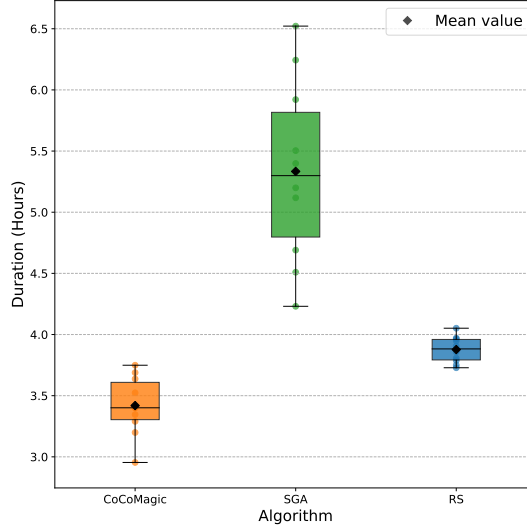


Fig. 14. Distribution of execution times (in hours) for *CoCoMagic*, *SGA*, and *RS* under a fixed search budget. Lower execution time indicates greater computational efficiency in completing the search. Each box summarizes the distribution of execution times across 10 runs.

Overall, the results for GP_2 exhibit similar trends to those observed for GP_1 , reinforcing the consistency of our findings across different MR groups.